IMPERIAL COLLEGE LONDON

Department of Earth Science and Engineering

Centre for Petroleum Studies

Sensitivity of Fractured Reservoir Performance to Static and Dynamic Properties, and History Matching

By

Stephen I. Chukwudi

A report submitted in partial fulfilment of the requirements for the MSc and/or the DIC.

September 2012

DECLARATION OF OWN WORK

I declare that this thesis

Sensitivity of Fractured Reservoir Performance to Static and Dynamic Properties, and History Matching

is entirely my own work and that where any material could be construed as the work of others, it is fully cited and referenced, and/or with appropriate acknowledgement given.

Signature:..

Name of student: Stephen I. Chukwudi

Name of supervisors: Professor Olivier R. Gosselin, and Dr. Thomas Schaaf (GDF-Suez)

Acknowledgements

I would like to express my sincere gratitude to God almighty, for seeing me through this project. I would also like to thank my supervisors Professor Olivier R. Gosselin and Dr. Thomas Schaaf for their guidance, support and useful suggestion throughout this project. Special thanks to SPDC Nigeria for sponsoring my MSc course at Imperial College London.

I express my sincere gratitude to my colleagues and friends from the Earth Science and Engineering Department especially Jhonatan Valdiviano Huertas, Benoit Decroux, Olufisayo Fagbowore, Morakinyo Apampa, Hammed Olanrewaju Bakare and Mathew Mancha for their support during the year. Finally, I thank my parents, brother, and sisters for their encouragement and support.

Table of Contents

List of Figures

List of Tables

List of Tables - Appendices

MSc in Petroleum Engineering 2011-2012

Imperial College London

Sensitivity of Fractured Reservoir Performance to Static and Dynamic Properties, and History Matching

Stephen I. Chukwudi

Professor Olivier R. Gosselin, Imperial College and Dr. Thomas Schaaf, GDF-Suez

Abstract

Sensitivity analysis is a key element for uncertainty quantification, and is the basis for further reduction of parameter uncertainty during history-matching. This is particularly crucial for naturally fractured reservoir (NFR). NFR have received much attention in the last decades because of low oil recovery in many of these reservoirs, and because of the potential to improve oil recovery from such reservoirs. NFR are highly heterogeneous and complex and in most case, the fluid flow characteristics are largely controlled by the fracture network properties. Thus, knowing the most sensitive fracture properties to cumulative oil production, length of plateau, and cumulative water production could be useful in making intelligent decisions during history matching.

This work presents a standard workflow for upscaling and simulating NFR, performing sensitivity study of fracture properties (such as fracture density, fracture length, orientation and aperture), and also suggests possible best practices during history matching. The Plackett-Burman design was used to analyze the most significant small scale fracture parameters to cumulative oil production, length of plateau, and cumulative water production. These fracture parameters with significant effect on field performances could be adjusted to get a better model during history matching and also preserved the geological consistency.

Introduction

About 30% of the world's oil and gas reserves are present in naturally fracture reservoirs (NFR). Most carbonate reservoirs (about 85%) are fractured. NFR have received much attention in the last decade because of low oil recovery in many of these reservoirs, and the potential to improve oil recovery from such reservoirs (Gang and Kelkar 2006). Fractured reservoirs are contradictory, with wide range of productivity and recovery. NFR are highly heterogeneous and complex and the fluid flow characteristics are largely controlled by the fracture properties, while the matrix properties also play a role in determining the production mechanisms. A naturally fractured reservoir can be classified into four types according to (Nelson 2001); Type I: Fractures provide the essential storage capacity and permeability in a reservoir. The matrix has little porosity or permeability. Type II: Rock matrix provides the essential storage capacity and fractures provide the essential permeability in a reservoir. The rock matrix has low permeability, but may have low, moderate, or even high porosity. Type III: Fractures provide a permeability assist in an already economically producible reservoir that has good matrix porosity and permeability. Type IV: Fracture does not provide significant additional storage capacity or permeability in an already producible reservoir, but instead create anisotropy (Barriers to flow). Fractures are mechanical discontinuities in a rock and may not be identified during the early life of the field. An optimal reservoir management requires accounting for the fracture effects as soon as possible in the reservoir development. Fractures in reservoir can either favour recovery or stop recovery prematurely with an early water breakthrough due to flows bypassing the matrix.

The use of a single-porosity simulator to model a naturally fractured reservoir can yield totally different results from those obtained from an appropriate fractured reservoir simulator (Sonier, Souillard et al. 1988). The accurate simulation of fractured reservoir is necessary in making key decision in such reservoir. Two well-known modelling approaches commonly used in simulating flow in fractured reservoirs are dual-porosity (DP) at a full field scale, and discrete fracture-network at a small scale (Jafari and Babadagli 2009). In the DP models, two different overlaid media are considered: matrix and fracture (Warren and Root 1963). DP models are limited in capturing the complex structure of fracture networks because they are based on a simplified description of matrix/fracture structure; however, they are useful, and perform better in describing the complex structure of fracture network than an homogenised model (Jafari and Babadagli 2009). Discrete fracture-network (DFN) approach is an efficient and accurate way to model fracture flow in fractured reservoirs. DFN and DFM (Discrete Fracture and matrix) models are more efficient and accurate in addressing the connectivity and scale dependent heterogeneity of fractured reservoirs compared to the DP models (Dershowitz, LaPointe et al. 2000), but they are restricted to small scale simulation, as they are computationally time-consuming.

DFN can be generated from both stochastic and deterministic modelling. Deterministic modelling is used when there are good information of where and how the fractures behave in 3D grid (Schlumberger 2007). If no such data are available, stochastic modelling is used. The fracture permeabilities can be upscaled analytically (Oda's method) or numerically (flow based method). Analytical methods of upscaling, which are mostly used due to computational efficiency, are limited to well connected fracture networks (fractures are supposed to be of infinite length). Flow based methods of upscaling, takes account of the full geometry of the system, but the calculations are much slower. In this work, the analytical method of upscaling was used, since the fractures are well connected.

Sensitivity analysis which is a key element for uncertainty quantification, and is the basis for further reduction of parameter uncertainty through history-matching is crucial in NFR. The aim of this study is to develop a complete workflow from fracture modelling to flow simulation during upscaling, analyse the most sensitive parameters to the production of a naturally fractured reservoirs, and also, suggest some best practices to design an efficient history matching strategy for fractured reservoir, with a feedback loop to the discrete scale fracture properties. Sensitivity analysis will be performed using Plackett-Burman designs to determine the fracture parameters that have significant effect on cumulative oil production, length of plateau, and cumulative water production. Then, the objective function (measuring the mismatch) could be minimized during history matching by adjusting theses parameters with significant effect.

Model Description

The geological model used in this work is a 3D synthetic grid based model (Cf. Cottereau et al., 2010). The reservoir grid and properties was imported to Petrel. The grid is faulted with 8 layers, averaging cell dimensions of 50×50×8 m (total number of cells: 20000). The model has 3 production wells and 3 injection wells. The matrix permeability in the x-direction range from 0.0005mD to 650mD, the permeability in the y-direction range from 0.0001mD to 215mD, the permeability in the z-direction range from 0 to 68mD and the porosity range from 0.4% to 23%, with an average value of 7%. The spatial distribution of porosity is related to three main facies (tight limestone, low porous limestone and porous limestone). The length of the reservoir is 2500m in the x-direction, 2500m in the y-direction and the height is about325m. The rock is water-wet. The model used in this work is the same model used by (Cottereau et al., 2010), but in this work, only a sector of it was consider due to software limitations. The aperture was change from 1cm in (Cottereau et al., 2010) to 0.05mm-0.15mm, which is a common range of aperture for fractured reservoirs.

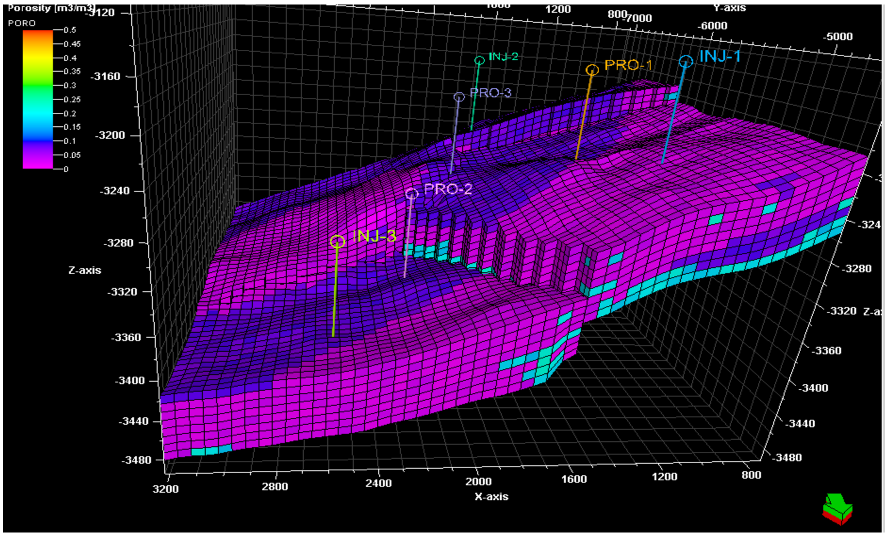

Figure 1: Geometry of the reservoir grid- Matrix porosity property display

Rock and Fluid Properties

Light oil and gas model was selected in Petrel, with reference pressure of 400 bars and temperature of 100°C. The oil-water contact was set below the reservoir model at a depth of 3,500m, and the gas-oil contact was set above the reservoir model at a depth of 3,000m. The reservoir lies between 3,168m and 3,493m deep. The bubble point pressure was set at 300 bars and the rock compressibility was set at 5.5E-5 bar-1 at a reference pressure of 400 bars. The gas, oil, and water density was set at 0.8 kg/m3, 800 kg/m3, and 1020 kg/m3 respectively. The oil-water relative permeability, gas-oil relative permeability, water-oil capillary pressure, and gas-oil capillary pressure was imported to Petrel.

Methodology and Direct Workflow

Discrete Fracture Network

The DFN generated in this work is based on a stochastic modelling. Three different fracture sets (NS, N120, and N70) were defined. The fracture density ranges from 0.05-1 (fracture area/volume), the fracture length range from 80 m-200 m, the aperture is defined by an exponential distribution and ranges from 0.05 mm-0.15mm. The orientation is defined by Fisher distribution, with a concentration factor which ranges from 10 to 40. The permeabilities of the DFN are correlated to the apertures with the cubic law.

Table 1: Orientation of three fractures set.

Fracture Set	Orientation Mean dip (°)	Orientation Mean dip-azimuth (°)
NS	88.1	95.4
N120	87.1	30.4
N70	88.6	340.6

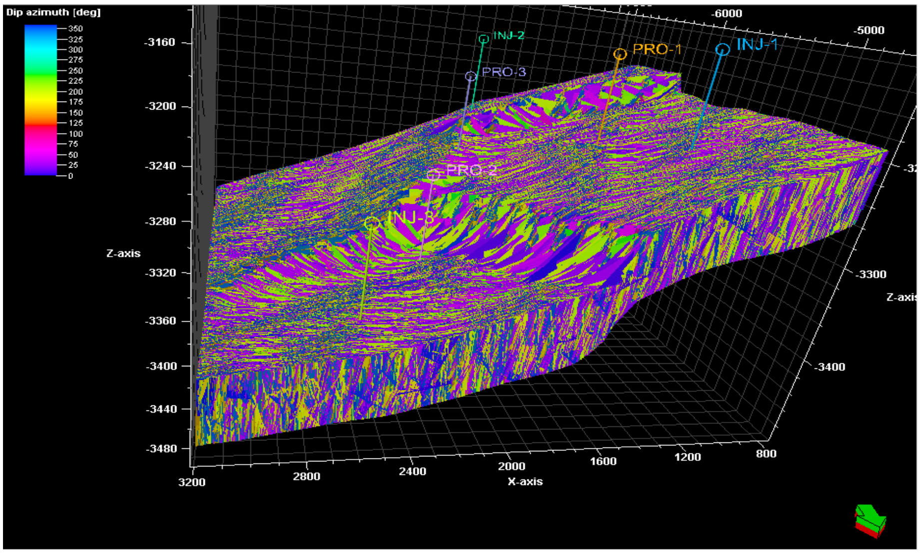

Figure 2: Geometry of DFN-Dip azimuth display

Equivalent Permeability Calculation

The fracture network effective permeability was computed, using the Oda's analytical method (ODA 1985). This method suggests that; if a fractured (cracked) rock mass can be assumed to be a homogenous, anisotropic porous medium, it obeys Darcy's law in which the apparent seepage velocity $\bar{v}_i$ is related to the gradient $-\frac{\partial\varphi}{\partial x_j}$ of total hydraulic head φ through a linking coefficient k_{ij} called the permeability tensor

$$\bar{v}_i = \frac{g}{v} k_{ij} j_j \quad \ldots (1)$$

Where g is the gravitational acceleration, v is the kinematic velocity and j_j is $-\frac{\partial\varphi}{\partial x_j}$

The equivalent permeability tensor $k_{ij}^{(f)}$ responsible for the fracture system is given as

$$k_{ij}^{(f)} = \frac{1}{12}\left(P_{kk}\delta_{ij} - P_{ij}\right) \quad \ldots (2)$$

Where

$$P_{ij} = \frac{\pi\rho}{4}\int_0^\infty \int_0^\infty \int_\Omega r^2 t^3 n_i n_j E(n,r,t)\, d\,\Omega\, dr dt \quad \ldots (3)$$

$$P_{kk} = P_{11} + P_{22} + P_{33} \quad \ldots (4)$$

The Oda's solution can be calculated without requiring flow simulations, however, it does not take fracture size and connectivity into account and is therefore limited to well connected fracture networks. Considering this limitation, the Oda solution is potentially useful for upscaling fracture permeabilities (Dershowitz, LaPointe et al. 2000).

Flow Simulation and Development Strategy

Dual Porosity

The dual porosity simulator in ECLIPSE was used in this work. This method assumes that fluids exist in two interconnected system; the rock matrix, which provide bulk of the reservoir volume and the rock fractures, which are highly permeable. This method also assumes that fluid flow in the reservoir take place only in the fracture network with the matrix acting as sources. In the dual porosity run of ECLIPSE, the number of grid in the z-direction is doubled. ECLIPSE associates the first half of the grid with the matrix blocks, and the second half with the fracture blocks (Schlumberger 2011).

Matrix-Fracture Coupling
A matrix-fracture coupling transmissibility is needed to simulate flow between the matrix and the fracture network. The matrix-fracture coupling transmissibility is constructed in ECLIPSE automatically to simulate flow between two systems due to fluid expansion, gravity drainage, capillary pressure etc. (Schlumberger 2011). The shape factor σ can be related to the matrix block size, using the expression proposed by (Kazemi, JR et al. 1976)

$$\sigma = 4\left(\frac{1}{L_x^2} + \frac{1}{L_y^2} + \frac{1}{L_z^2}\right) \qquad (5)$$

Where $L_x, L_y, and\ L_z$ represent the X, Y, and Z dimensions of the matrix blocks.

The ECLIPSE keyword GRAVDRM was activated, this keyword account for fluid exchange between the fracture and the matrix due to gravity (Quandalle and Sabathier formulation). This formulation required two values of shape factor for each gridblock to model fluid flow transfer between matrix and fracture network in horizontal and vertical directions.

$$\sigma_h = 4\left(\frac{1}{L_x^2} + \frac{1}{L_y^2}\right) \qquad (6)$$

$$\sigma_{gd} = 2\left(\frac{1}{L_z^2}\right) \qquad (7)$$

$$d_{zmtrx} = L_Z \qquad (8)$$

σ_h is the horizontal shape factor
σ_{gd} is the vertical gravity drainage shape factor.

The ECLIPSE keywords SIGMAV, SIGMAGDV, and DZMTRXV were imported; SIGMAV is used to specify a multiplier to be applied in the construction of the matrix-fracture coupling transmissibilities, SIGMAGDV is used to specified an alternative matrix-fracture coupling for cells in which the production mechanism is gravity drainage due to the presence of gas in the fractures, and DZMTRXV is used to specify the vertical dimension of a typical block of matrix material. The values of SIGMAV computed by Petrel were not acceptable, so the values of SIGMAV, SIGMAGDV and DZMTRXV computed in Cottereau et al., 2010 was used.

Development Strategy
The well layout design to perform fluid flow simulation includes three producers and three injection wells. Water injection is scheduled to start one year later. The production wells are perforated from layer 1 to layer 5, and the injection wells are perforated from layer 5 to layer 8. The production scenario is constrained by the reservoir fluid volume rate (RESV). The reservoir volume rate target is set to 170rm3/d. The bottom hole pressure limits for production wells is set to 250 bars, at the reference depth of 3335 m. Water injection is controlled by the surface flow rate; the surface flow rate is set to 200 sm3/d and the bottom hole pressure is set to 450 bars. Production is scheduled to start on January 1st, 2012 to January 1st, 2025. Water injection is scheduled to start on January 1st, 2013 to January 1st 2025.

Sensitivity and inverse workflow

Workflow Summary
This work proposed the workflow below (Fig. 3) for the modeling of fracture reservoir. It is important to note here that the geological model was not upscale, since it's a sector model. Only the DFN properties was upscale.

Parameterisation
In this work, four fracture parameters (length, density, orientation concentration, and aperture) were tested in a model with three fracture sets, making a total of 12 variables.

Experimental Design
The Plackett-Burman designs were used to access the most significant fracture parameters to cumulative oil production, length of plateau, and cumulative water production. These designs were proposed by (Plackett and Buman 1946). These designs allow the estimation of main effect using limited number of runs when compared to other designs.
The Plackett-Burman designs require 16 runs to estimate the most significant variables. DOE++, which is an experimental design software from Reliasoft was used in this work.

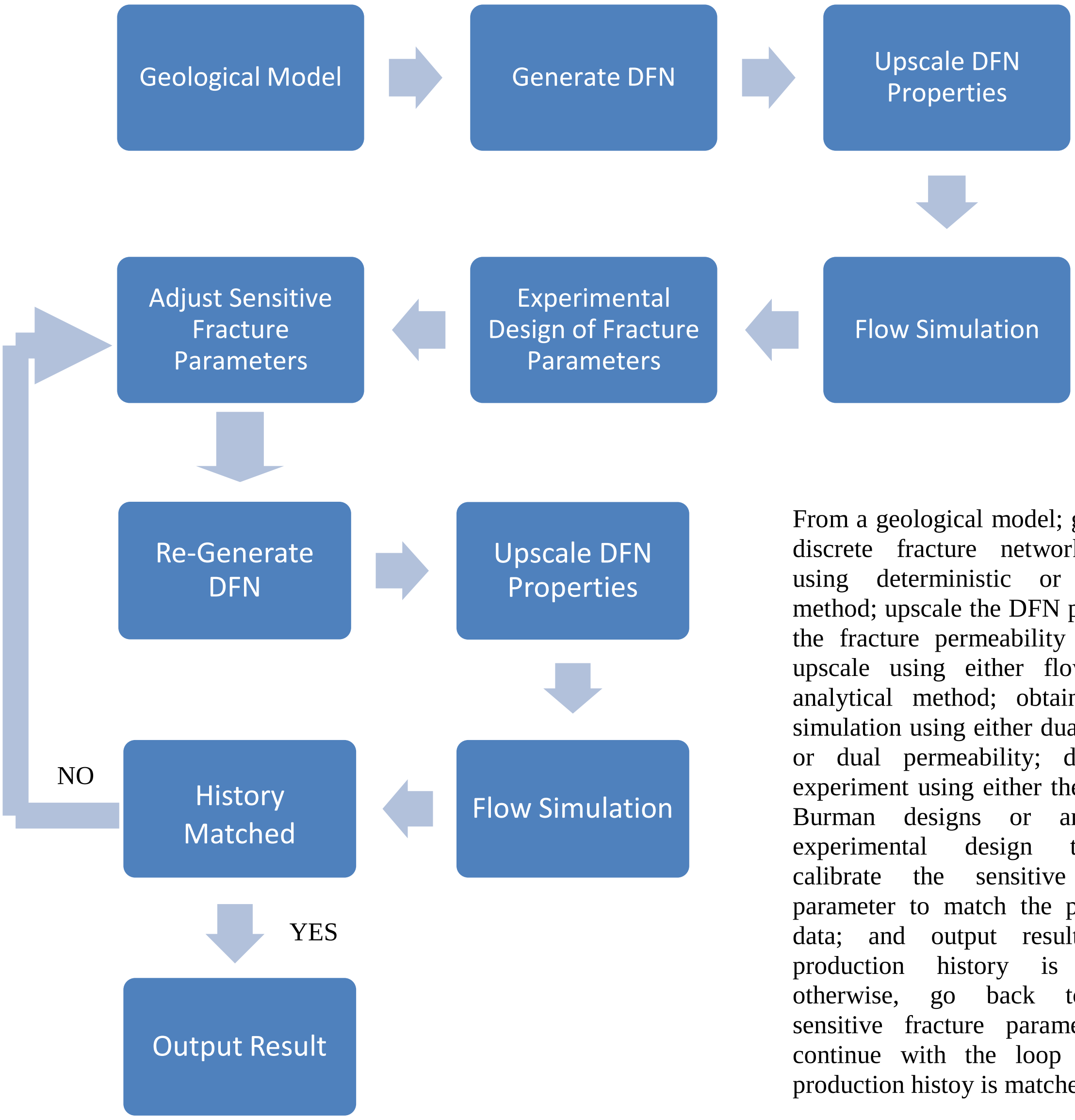

From a geological model; generate a discrete fracture network (DFN) using deterministic or stocastic method; upscale the DFN properties, the fracture permeability could be upscale using either flowbase or analytical method; obtain a flow simulation using either dual porosity or dual permeability; design an experiment using either the Plactett-Burman designs or any other experimental design technique; calibrate the sensitive fracture parameter to match the production data; and output result if the production history is matched otherwise, go back to adjust sensitive fracture parameters and continue with the loop until the production histoy is matched

Figure 3: Workflow proposed by this work for modelling fractured reservoirs.

Sensitivity Analysis Results

Cumulative oil production, length of plateau, and cumulative oil production were obtained from 16 runs. The purpose of this was to access the impact of four fracture parameters (Length, density, orientation, and aperture) on the cumulative oil production, length of plateau, and cumulative water production in the three fracture set. This is important because it will enable us to make intelligent decisions on the variable(s) to tune during history matching. The Plackett-Burman designs were set up. The tables below show the high and low values used in the experiment for each fracture parameter in the three fracture sets.

Table 2: High and low value for fracture density, length, and aperture

Fracture Set	Fracture Density (Fracture area/volume)		Aperture (mm)		Fracture Length (m)	
	Low	High	Low	High	Low	High
NS	0.05	0.1	0.05	0.15	80	200
N120	0.1	0.5	0.05	0.15	80	200
N70	0.5	1	0.05	0.15	80	200

Table 3: Orientation with high and low value of concentration factor

Fracture Set	Orientation Mean dip (°)	Orientation Mean dip-azimuth (°)	Concentration factor, K	
			Low	High
NS	88.1	95.4	40	10
N120	87.1	30.4	40	10
N70	88.6	340.6	40	10

The orientation was defined by Von Mises-Fisher distribution. The concentration factor (Fisher constant, k) was change to give two set of orientation, as shown in table 3 above. The orientation with concentration factor of 10 represent the high case and concentration factor of 40 represent the low case.

Table 4: Coded Plakett-Burman design matrix of 16 runs for 12 variables with results

Run Order	D1	L1	C1	A1	D2	L2	C2	A2	D3	L3	C3	A3	Cumulative Oil Production (sm3/d)	Length of Plateau (months)	Cumulative water production (sm3/d)
1	1	-1	1	-1	1	1	-1	-1	1	-1	-1	-1	24553	0	6.9
2	-1	1	1	-1	-1	1	-1	-1	-1	1	1	1	122125	0	27.6
3	1	-1	-1	1	-1	-1	-1	1	1	1	1	-1	90735	0	21.6
4	-1	-1	1	-1	-1	-1	1	1	1	1	-1	1	362802	33	76.4
5	1	1	-1	-1	1	-1	-1	-1	1	1	1	1	410494	66	84.7
6	1	1	1	1	-1	1	-1	1	1	-1	-1	1	397758	72	79.1
7	-1	-1	1	1	1	1	-1	1	-1	1	1	-1	185080	0	41.9
8	-1	1	-1	1	1	-1	-1	1	-1	-1	-1	1	401152	60	76.2
9	-1	1	1	1	1	-1	1	-1	1	1	-1	-1	49430	0	13
10	-1	1	-1	-1	-1	1	1	1	1	-1	1	-1	48680	0	12.8
11	1	-1	-1	-1	1	1	1	1	-1	1	-1	1	357868	32	73
12	1	1	-1	1	-1	1	1	-1	-1	1	-1	-1	28634	0	8
13	-1	-1	-1	-1	-1	-1	-1	-1	-1	-1	-1	-1	7879	0	2.5
14	-1	-1	-1	1	1	1	1	-1	1	-1	1	1	409187	68	24
15	1	1	1	-1	1	-1	1	1	-1	-1	1	-1	135713	0	31
16	1	-1	1	1	-1	-1	1	-1	-1	-1	1	1	174790	0	39

D1=Fracture density (Fracture area/volume) for NS, L1=Fracture length (m) for NS, C1=Concentration factor for NS, A1=Aperture (mm) for NS
D2=Fracture density (Fracture area/volume) for N120, L2=Fracture length (m) for N120, C2=Concentration factor for N120, A2=Aperture (mm) for N120
D3=Fracture density (Fracture area/volume) for N70, L3=Fracture length (m) for N70, C3=Concentration factor for N70, A3=Aperture (mm) for N70

NS=First fracture set N170=Second fracture set N70=Third fracture set

Table 4 above represents a coded Plakett-Burman design of 16 runs for 12 variables and the corresponding response variables for each run. 1and -1 represents a high and low value respectively for each fracture parameter. The 16 runs were done in ECLIPSE and the results were exported to DOE++ for sensitivity study.

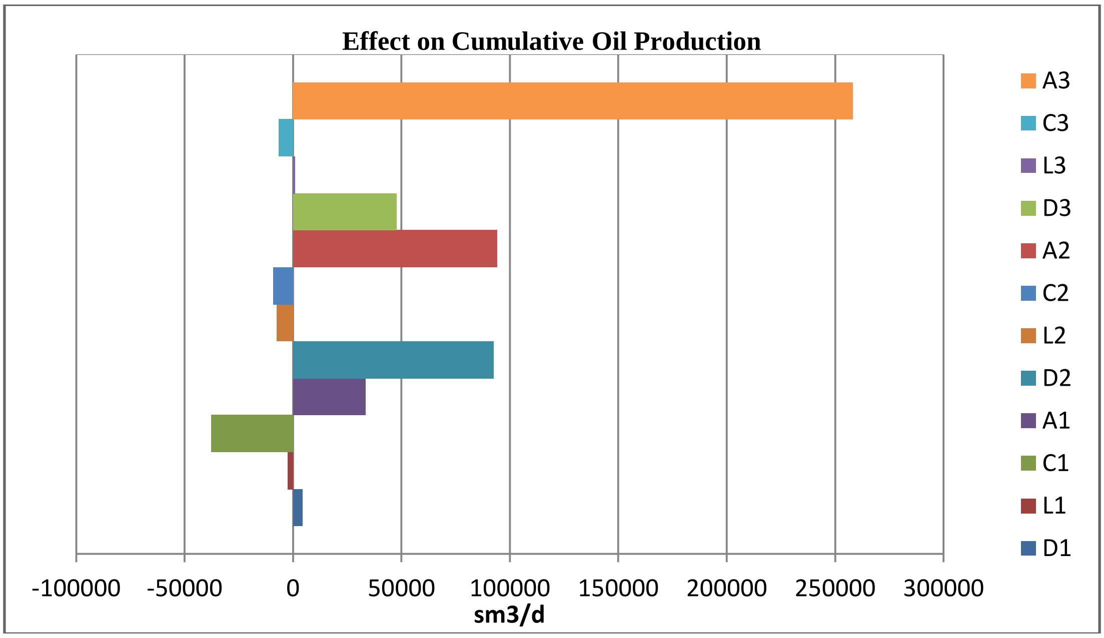

Figure 4: Effect of facture parameters on cumulative oil production.

Figure 4 above, shows the positive and negative effect on cumulative oil production, caused by different fracture parameters in the three fractures sets. This chart is useful during history matching. It shows which parameter to increase or reduce to get a good match.

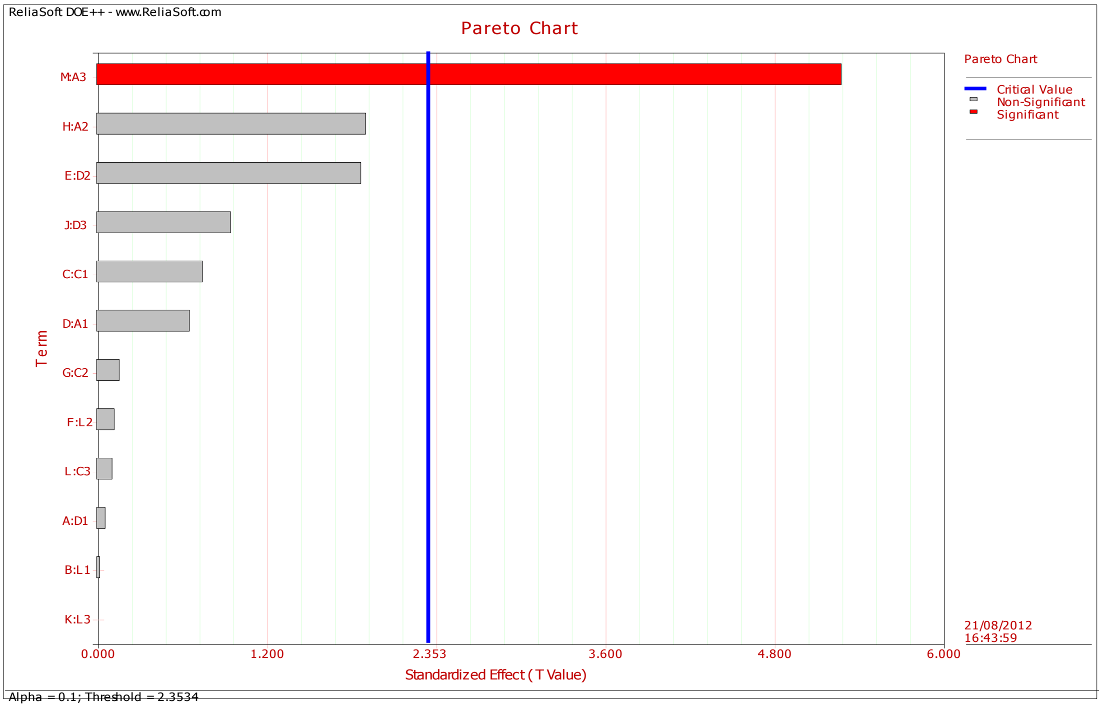

Figure 5: Pareto chart, showing the fracture parameter with the most significant effect on cumulative oil production.

From figure 5 above, we observed that the fracture aperture (A3) in the third fracture set (N70) has a significant effect on cumulative oil production. We also observed that, as the high and low value of fracture in each fracture set density increases, the effect of the fracture aperture also increases. This information is very useful during history matching.

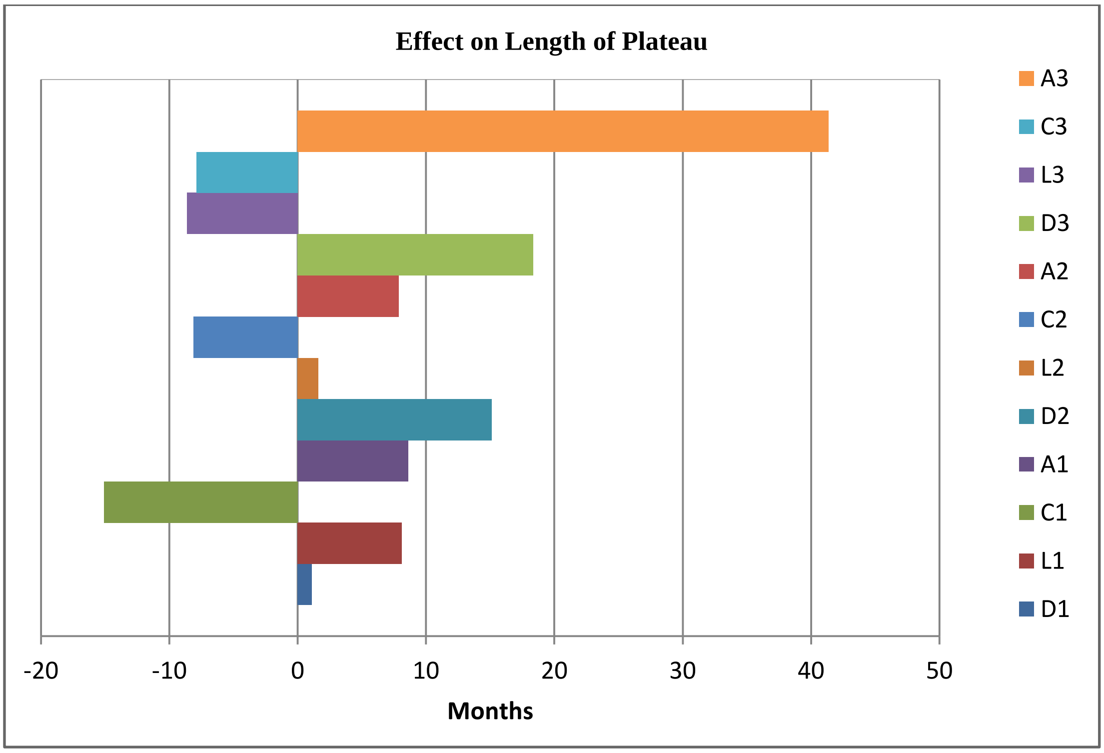

Figure 6: Effect of facture parameters on the length of plateau.

Figure 6 above, shows the positive and negative effect on the length of plateau, caused by different fracture parameters in the three fractures sets.

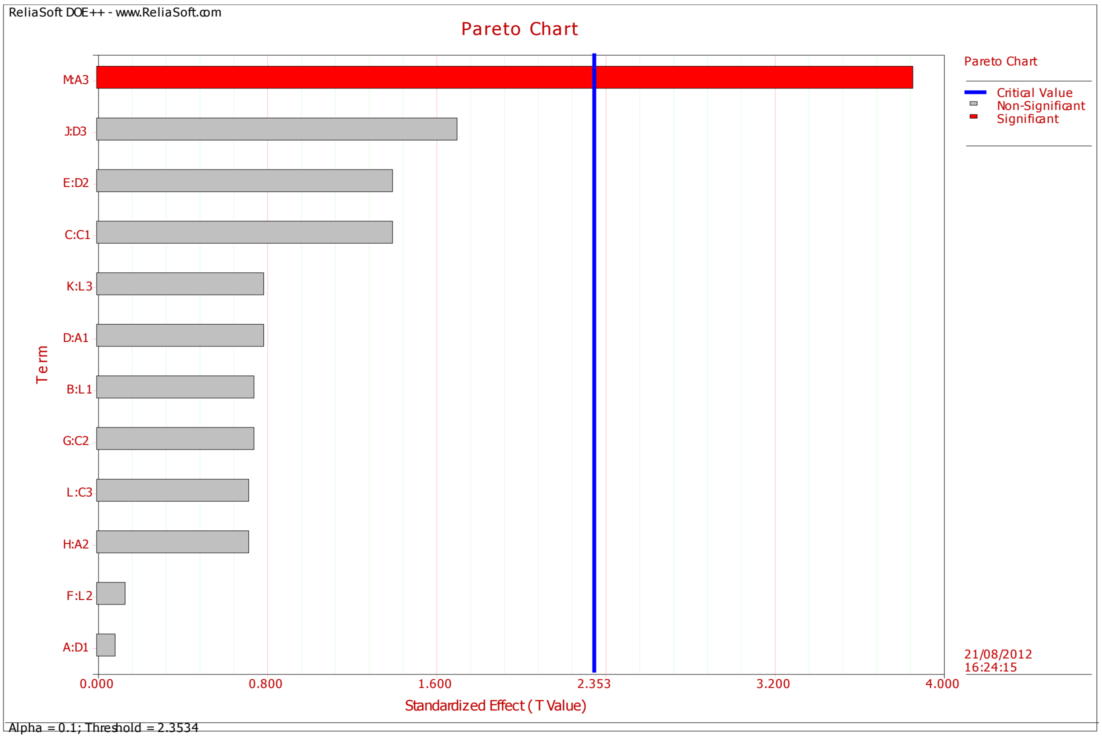

Figure 7: Pareto chart, showing the fracture parameter with the most significant effect on the length of plateau.

From figure 7, the fracture aperture (A3) in the third fracture set (N70) has a significant effect on the length of plateau.

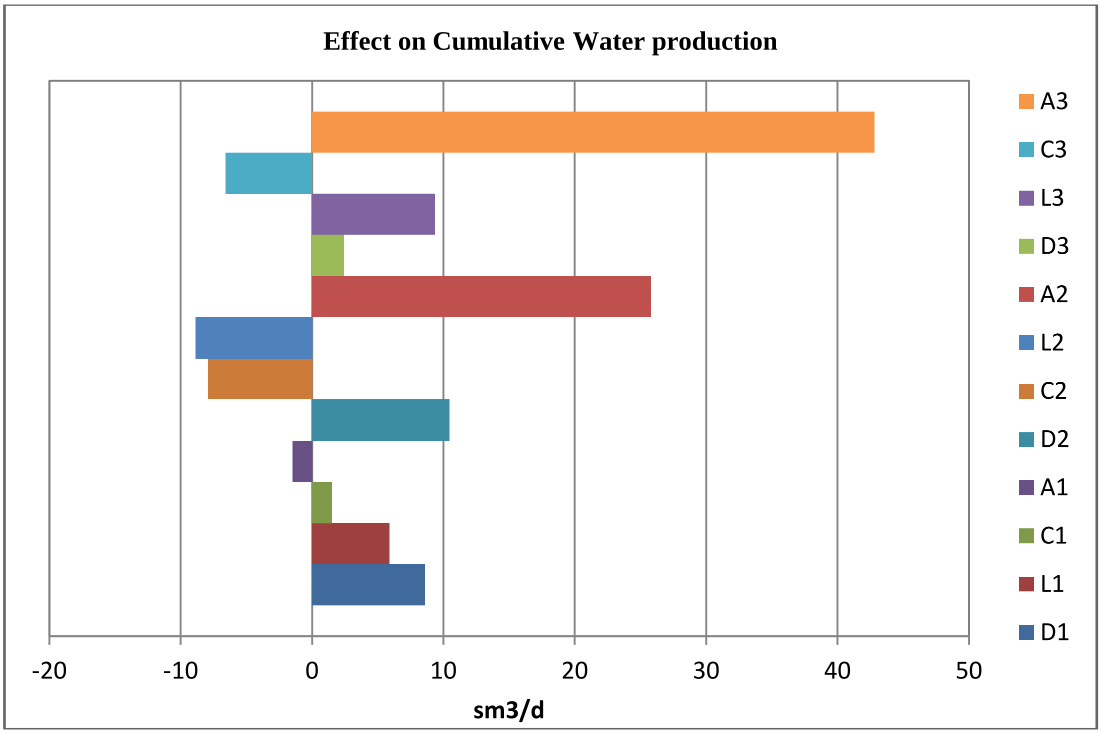

Figure 8: Effect of facture parameters on cumulative water production

Figure 8 above, shows the positive and negative effect on cumulative water production, caused by different fracture parameters in the three fractures sets.

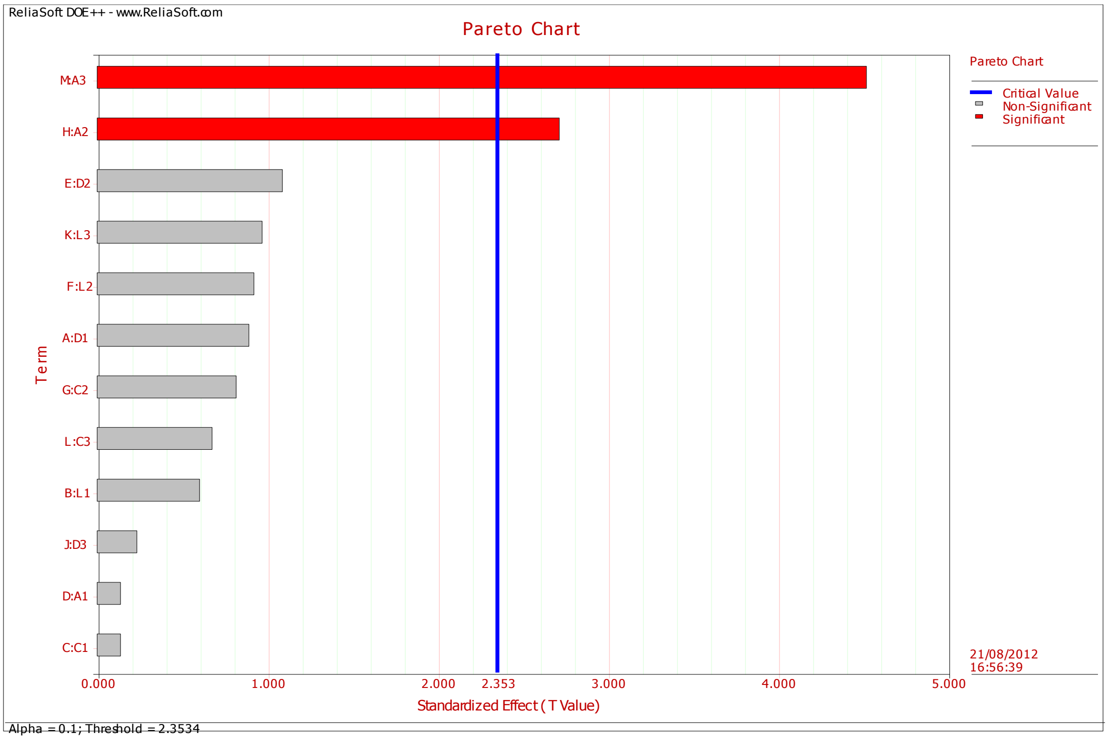

Figure 9: Pareto chart, showing the fracture parameter with the most significant effect on cumulative water production.

From figure 9, the fracture aperture in the third and second (N120) fracture set has a significant effect on the cumulative water production.
From the results above, the fracture aperture A3 of the third fracture set N70 has the most significant effect on cumulative oil production, length of plateau, and cumulative water production. The focus of this work from this point, is find out if we can get a good history match by tuning the fracture aperture of the third fracture set.

History Matching

In this work, in order to test some history-matching strategy, we defined a “true case as follows:

Table B - 1: Values of fracture parameter for true case.

Fracture Set	Density (Frac area/volume)	Length (m)	Concentration	Aperture (mm)
1	0.08	150	20	0.00013
2	0.3	150	20	0.00013
3	0.85	150	20	0.00013

The development strategy is the same as the one used in the matched case below, the reservoir volume is 180 rm3/d, and water injection started the same year with production (from January 2012 to January 2016). The observed data was the simulated results from this “true” synthetic case.

The history matching approach proposed in this work is to calibrate the most sensitive fracture parameter with the production data. This approach preserves the geological consistency during history matching. The conventional history matching approach based on the direct adjusting of effective permeability in the gridblock tends to lose consistency with the static fracture distribution model (Gang and Kelkar 2006).

Objective function

History matching involves the minimization of an objective function, which represents the mismatch between the observed and simulated data. The root mean square was used in this work to calculate the match value. This is given as;

$$M(x) = \sqrt{\frac{1}{N}\sum_{i=1}^{N}\left(\frac{S_i(x) - O_i}{\sigma_i}\right)^2} \quad \ldots \ldots \ldots \ldots (9)$$

M is the match value.
N is the number of points used to compute M.
S_i is the simulated value.
O_i is the observed value.
x is the model parameter vector
σ_i is a normalization parameter, e.g. the measurement error associated to observation i. (Schlumberger Petrel 2010)

Simulation 4 in the Plackett-Burman design was chosen as the initial simulation; the observed data was imported to Petrel, and a matched model was obtain by tuning only the aperture A3 in the third fracture set (N70), as a results of the sensitivity study. The match value was minimized by reducing the value of aperture A3 in N70 from 0.15mm to 0.141mm. The strategy was also edited to minimize the match value; the reservoir volume was increase from 170rm3/d to 180rm3/d, and water injection started the same year with production (from January 2012 to January 2016).

Table 5: Values of fracture parameter for initial and matched simulation.

	D1	L1	C1	A1	D2	L2	C2	A2	D3	L3	C3	A3
Initial	0.05	80	10	0.05	0.1	80	10	0.15	1	200	40	0.15
Matched	0.05	80	10	0.05	0.1	80	10	0.15	1	200	40	0.141

Table 5 above show the values of the fracture parameters in the initial simulation and matched simulation. The only different in the initial and matched is the value of aperture in N70. This shows the important of the sensitivity study.

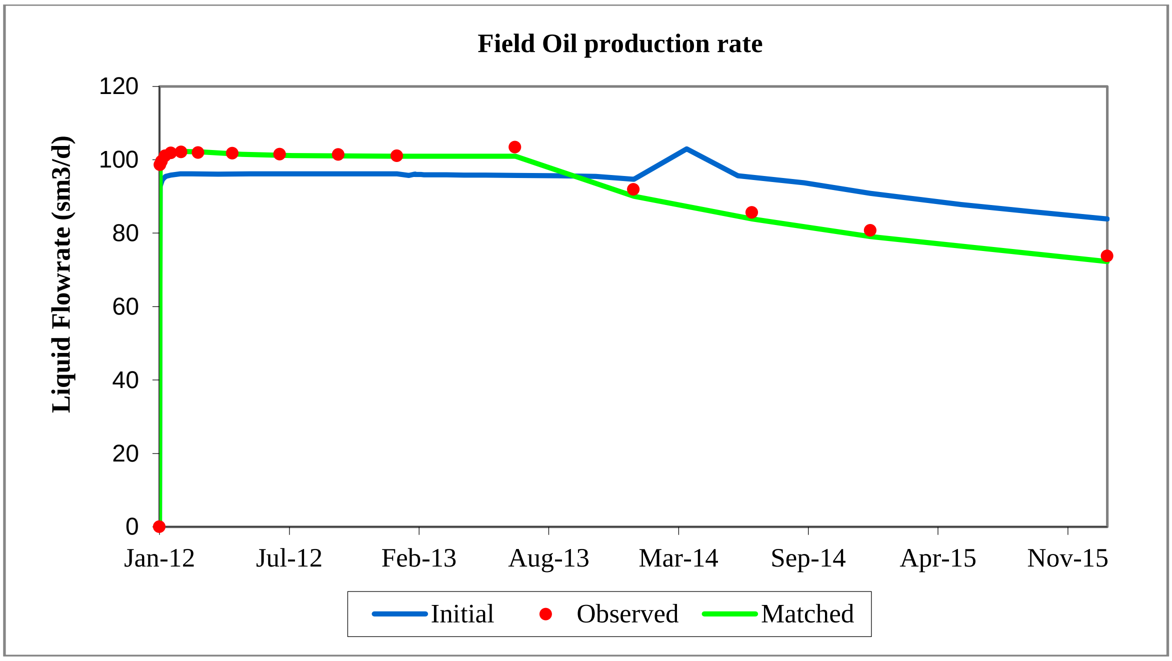

Figure 10: Match result for field oil production.

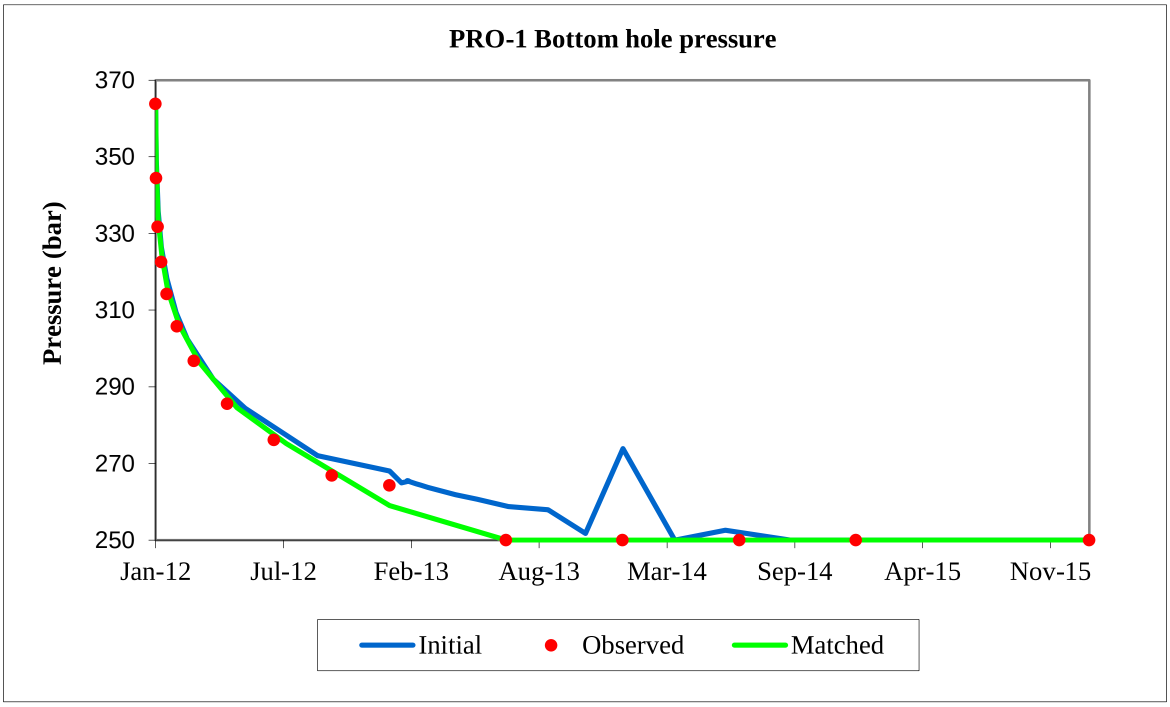

Figure 11: BHP match result for production well 1 (PRO-1).

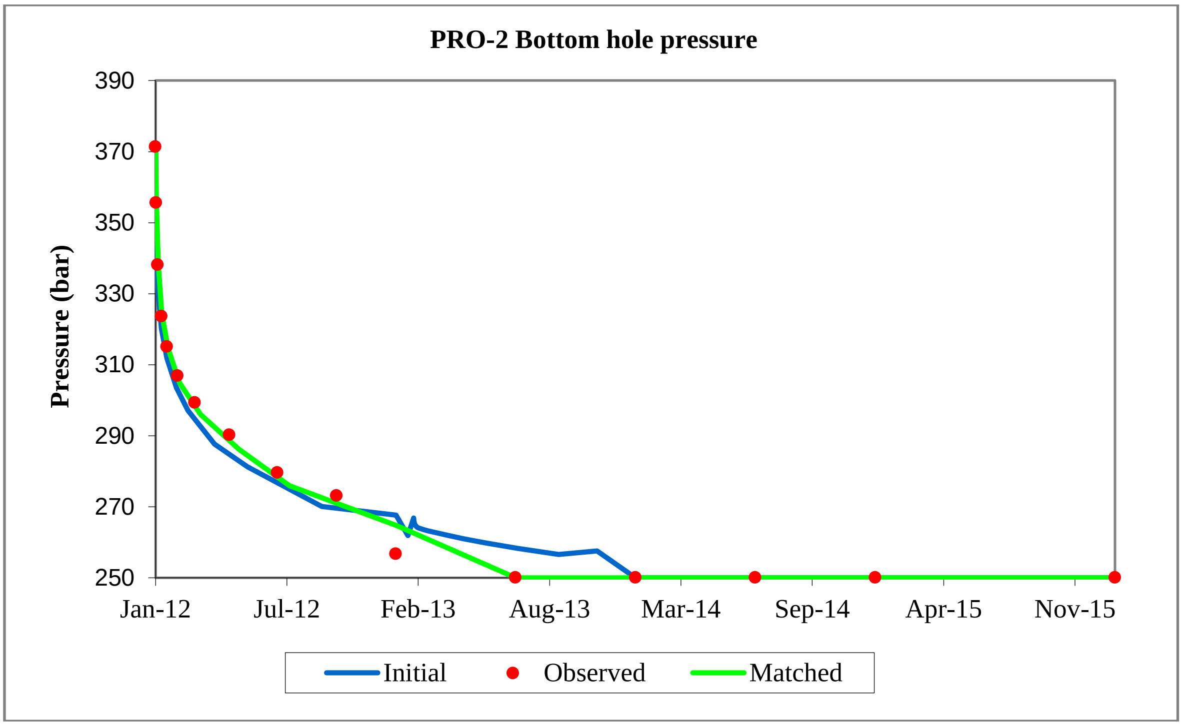

Figure 12: BHP match result for production well 2 (PRO-2).

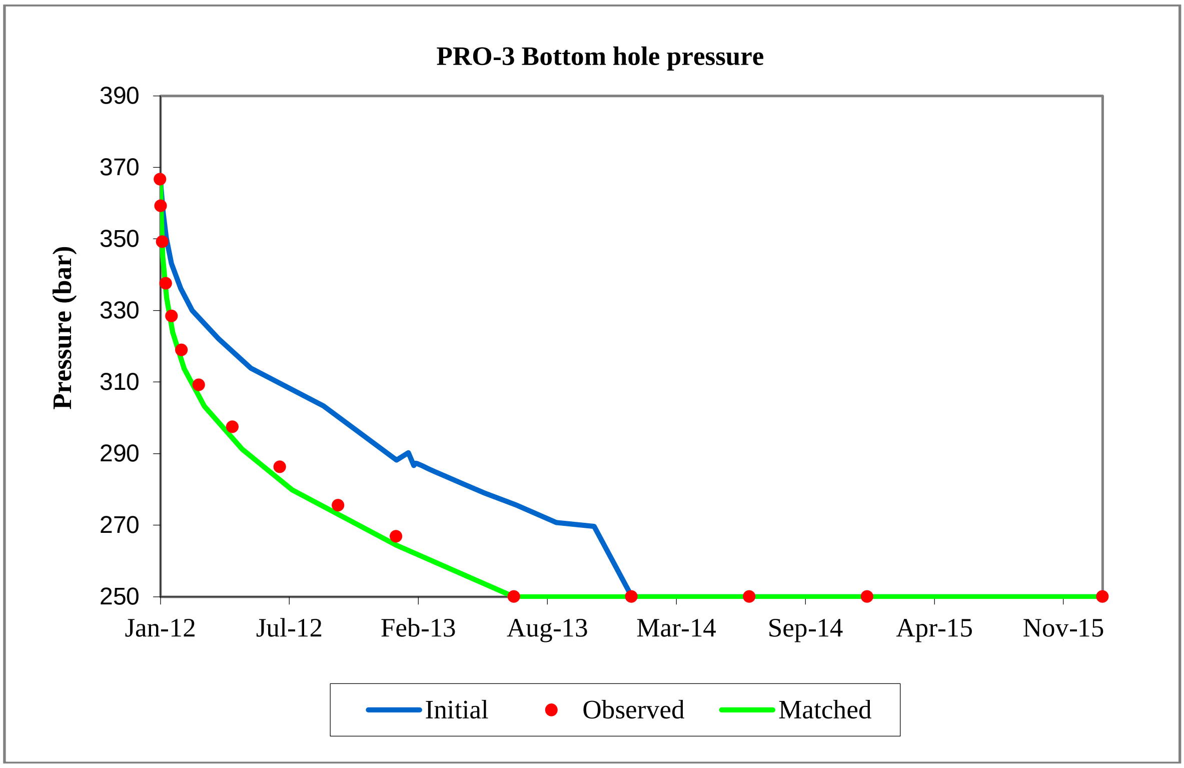

Figure 13: BHP match result for production well 3 (PRO-3).

The field oil production and the bottom hole pressure was matched by calibrating the aperture A3 in the N70, which is the fracture parameter that has the most significant effect on cumulative oil production, length of plateau and cumulative water production as shown above. Thus, the sensitivity study enables us to reduce parameter uncertainties and enable us to focus on the parameter(s) with high effect during history matching.

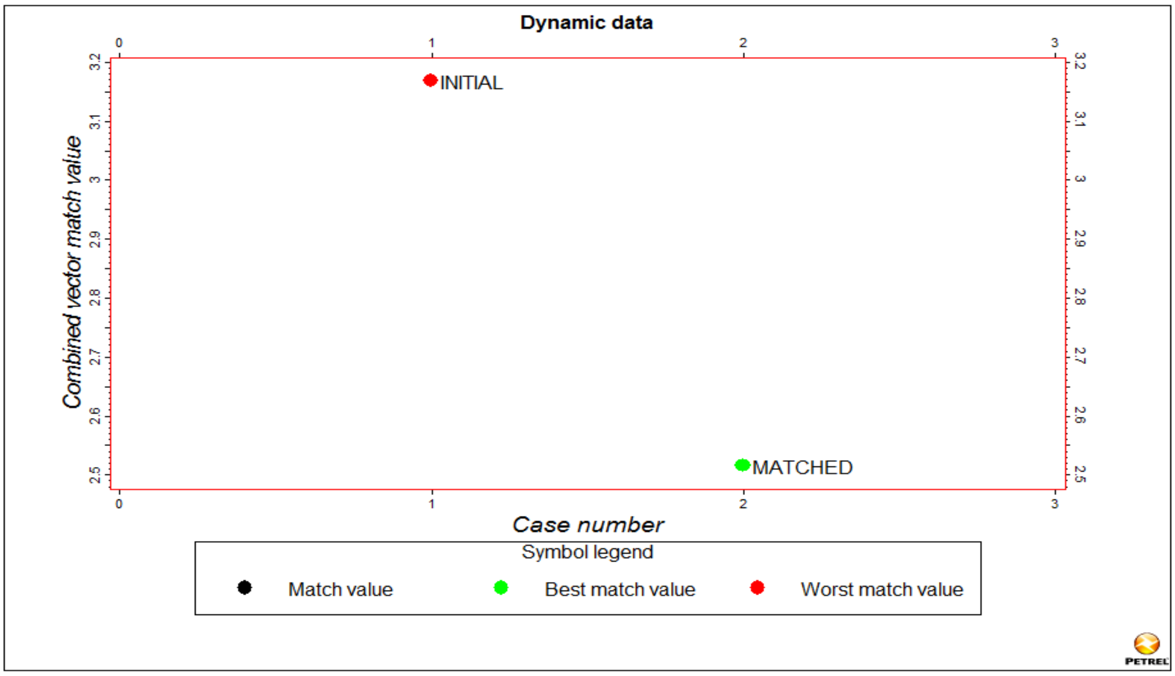

Figure 14: Match value for initial and matched simulation.

From figure 14, the match value was reduced from about 3.2 to 2.5 by calibrating the fracture parameter with the most significant effect to match the production data. This method of history matching is very useful because it preserves the model geological consistency.

Conclusions

This work proposed a direct workflow for modelling naturally fracture reservoirs, starting from the properties of the discrete fracture network to the simulated field performances, through upscaling from discrete properties to continuous dual-medium model parameters.
A sensitivity analysis using experimental design was suggested and performed to determine the fracture parameter(s) with significant effect on cumulative oil production, length of plateau, and cumulative water production. This step of experimental design allows reduction of the number of parameters to be calibrated.
On this basis, an inverse workflow was proposed to adjust the most sensitive fracture parameters, at the discrete scale, instead of adjusting gridblock permeability, in order to get a better match with history production data.
It is expected that the geological consistency can be preserved through the approach proposed in this work.

Recommendations for Further Study

The extent of this work was limited by time constraints. Thus, the following aspects required further study: A further study could be done using this approach on a full field. The value of aperture used in this work is between 0.05mm and 0.15mm. Thus, a higher range of aperture could be interesting since the aperture has the most significant effect in this work. The Plakett-Burman designs were used in this work to obtain the fracture parameter with the most significant effect. A further study can be done using general full factorial design, where each fracture parameter can have more than two levels and also, the interaction between the fracture parameter can be measure.

Nomenclature

L_x	X dimensions of the matrix blocks
L_y	Y dimensions of the matrix blocks
L_z	Z dimensions of the matrix blocks.
O_i	Observed value.
S_i	Simulated value.
σ_h	Horizontal shape factor
σ_{gd}	Vertical gravity drainage shape factor
σ_i	Normalization parameter,
BHP	Bottom hole pressure
DFN	Discrete fracture network
DP	Dual porosity
Kg/m3	Kilogram per meter cube
M	Match value.
m	meter
mD	Milli-darcy
mm	millimeter
N	Number of points used to compute M
NFR	Naturally fracture reservoirs
RESV	Reservoir volume
Sm3/d	Standard cubic meter per day
x	Model parameter vector
σ	Kazemi shape factor

References

Dershowitz, B., P. LaPointe, et al. (2000). "Integration of Discrete Feature Network Methods With Conventional Simulator Approaches." SPE 62498 presented at the 1998 SPE Annual Technical Conference and Exhibition, New Orieans, 27–30 September **3**(2): 165-170.

Gang, T. and M. Kelkar (2006). "History Matching for Determination of Fracture Permeability and Capillary Pressure." SPE 101052 Presented at the 2006 SPE Annual Technical Conference and Exhibition held in San Antonio, Texas, U.S.A., 24-27 September 2006.

Jafari, A. and T. Babadagli (2009). "A Sensitivity Analysis for Effective Parameters on 2D Fracture-Network Permeability." SPE 113618 Presented at the SPE Western regional and Pacific Section AAPG Joint Meeting, Bakersfield, Califonia, USA, 29 March-2 April 2008.

Kazemi, H., L. S. M. JR, et al. (1976). "Numerical Simulation of Water-Oil Flow in Naturally Fractured Reservoirs." SPE 5719 **16**: 317-326.

Nelson, R. A. (2001). Geological Analysis of Naturally Fractured Reservoirs.

ODA, M. (1985). "Permeability tensor for discontinuous rock masses."

Plackett, R. L. and J. P. Buman (1946). "The Design Of Optimum Multifactorial Experiments." Biometrika **33**(4): 296-304.

Schlumberger (2007). "Petrel Fracture Modeling."

Schlumberger (2011). "ECLIPSE Technical Description." Copyright © 1982 - 2011 Schlumberger.

Schlumberger (Petrel 2010). "Reservoir Engineering Course."

Sonier, F., P. Souillard, et al. (1988). "Numerical Simulation of Naturally Fractured Reservoirs." SPE 15627 presented at the 1986 SPE Annual Technical Conference and Exhibition held in New Orleans, Oct. 5-8: 1114-1122.

Warren, J. E. and P. J. Root (1963). "The behavior of Naturally Fractured Reservoirs." SPE 426 Presented at the Fall Meeting of SPE in Los Angeles on Oct. 7-10, 1962: 245-255.

Appendix

The ODA Analytical Method

This method suggests that; if a fractured (cracked) rock mass can be assumed to be a homogenous, anisotropic porous medium, it obeys Darcy's law in which the apparent seepage velocity $\bar{v}_i$ is related to the gradient $-\frac{\partial\varphi}{\partial x_j}$ of total hydraulic head φ through a linking coefficient k_{ij} called the permeability tensor

$$\bar{v}_i = \frac{g}{v} k_{ij} j_j \ldots\ldots\ldots (1)$$

Where g is the gravitational acceleration, v is the kinematic velocity and j_j is $-\frac{\partial\varphi}{\partial x_j}$
For impermeable matrix, since fluid only flows through the fractures, the apparent flow velocity v_i is defined by

$$\bar{v}_i = \frac{1}{V}\int_{V^{(f)}} v_i^{(f)} dV^{(f)} \ldots\ldots\ldots (2)$$

Where $v_i^{(f)}$ is the local velocity in the fractures and $V^{(f)}$ is the volume associated with the fractures

The probability density function $E(n,r,t)$is introduced in such a way that $2E(n,r,t)d\,\Omega\,drdt$ gives the probability of (n,r,t) fractures. It satisfies

$$\int_0^\infty\int_0^\infty\int_{\frac{\Omega}{2}} 2E(n,r,t)d\Omega drdt = \int_0^\infty\int_0^\infty\int_\Omega E(n,r,t)d\,\Omega\,drdt = 1 \ldots\ldots\ldots (3)$$

Let dN be the number of (n,r,t) fractures whose centres are located inside the flow region of volume V. To estimate the number, the probability of (n,r,t) fractures is multiplied by the total number $m^{(f)}$

$$dN = 2m^{(f)}E(n,r,t)d\Omega drdt \ldots\ldots\ldots (4)$$

Since each (n,r,t) fractures produces a void volume equal to$\left(\frac{\pi}{4}\right)r^2t$, the total void volume $dV^{(f)}$ associated with the (n,r,t) fractures is given by

$$dV^{(f)} = \frac{\pi r^2 t}{4}dN = \frac{\pi m^v}{2} r^2 tE(n,r,t)d\Omega drdt \ldots\ldots\ldots (5)$$

If the fractures extend indefinitely, the fluid movement can be idealized by laminar flow between parallel planar plates with an aperture t. The mean velocity $v_i^{(f)}$ is defined by

$$v_i^{(f)} = \frac{1}{12}\frac{g}{v}t^2 J_i^{(f)} = \frac{1}{12}\frac{g}{v}t^2\left(\delta_{ij} - n_i n_j\right)J_j \ldots\ldots\ldots (6)$$

Where δ_{ij} is the kronecker delta and n_i and J_j respectively are components of n and J projected on the orthogonal reference axis x_i $(i = 1,2,3)$.
Using equation (5) and (6), equation (2) becomes

$$\bar{v}_i = \frac{1}{12}\frac{g}{v}\left[\frac{\pi\rho}{4}\int_0^\infty\int_0^\infty\int_\Omega r^2t^2(\delta_{ij}-n_in_j)E(n,r,t)d\,\Omega\,drdt\right]J_j \quad (7)$$

Where ρ is the volume of fractures defined by

$$\rho = \frac{m^{(v)}}{V} \quad (8)$$

A comparison between equation (7) and (1), gives the equivalent permeability tensor $k_{ij}^{(f)}$ responsible for the fracture system.

$$k_{ij}^{(f)} = \frac{1}{12}\left(P_{kk}\delta_{ij} - P_{ij}\right) \quad (9)$$

Where

$$P_{ij} = \frac{\pi\rho}{4}\int_0^\infty\int_0^\infty\int_\Omega r^2t^3n_in_jE(n,r,t)d\,\Omega\,drdt \quad (10)$$

$$P_{kk} = P_{11} + P_{22} + P_{33} \quad (11)$$

The Oda’s solution can be calculated without requiring flow simulations, however, it does not take fracture size and connectivity into account and is therefore limited to well connected fracture networks

Appendix A: Literature Review

Table A- 1: Key Milestones Related to this Study

SPE Paper n°	Year	Title	Authors	Contribution
426	1963	"The behavior of Naturally Fractured Reservoirs"	J. E. Warren, P. J. Root.	An idealized model to study the characteristic behaviour of double porosity reservoir.
5719	1976	"Numerical Simulation of Water-Oil Flow in Naturally Fractured Reservoirs"	Kazemi H., Merrill L., Porterfield K., Zeman P	A three dimensional, multiple-well, numerical simulator for simulating single or two-phase flow of water and oil was developed for fractured reservoir.
12270	1983	"Simulation of Naturally Fractured Reservoirs"	Saidi A.M.	A three-dimensional, three-phase reservoir simulator was developed to study the behavior of fully or partially fractured reservoirs.
15627	1988	"Numerical Simulation of Naturally Fractured Reservoirs"	F. Sonier, P. Souillard, F. T. Blaskovich.	This paper present a new technique to simulate matrix/fracture exchange with special emphasis on the gravity forces included in the exchange terms
18427	1989	"Implicit Compositional Simulation of Single-Porosity and Dual-Porosity Reservoirs"	Coats, K. H.	Describe an implicit numerical model for computational simulation of single-porosity and dual-porosity oil or gas condensate reservoirs.
39825	1998	"A New Approach of Fractured Reservoirs"	Sabathier J.C., Bourbiaux B., Cacas M.C., Sarda S.	This paper describes the complete methodology and formulation, which could be input in other dual-porosity simulation.
62498	2000	Integration of Discrete Feature Network Methods With Conventional Simulator Approaches	B., Dershowitz, P., Lapointe, T., Eiben, L., Wei	This paper presents different techniques to develop Dual porosity models that more accurately reflect the anisotropy, heterogeneity, and scale dependent connectivity structure of fractured reservoirs
84078	2003	"Practical Approach in Modeling Naturally Fractured Reservoir: A Field Case Study"	Asnul B., Harun A., Maged H. A., Salem E. S., Hussein B., Mohan K	This paper presents a practical approach in modeling of naturally fractured reservoirs, from geology to flow simulation.
101052	2006	"History Matching for Determination of Fracture Permeability and Capillary Pressure"	T. Gang, M. Kelkar.	This paper presents an integrated approach to history matching naturally fractured reservoirs by adjusting the fracture permeability of individual fractures and water/oil capillary pressure curves.
107525	2007	"Fast and Efficient Modeling and Conditioning of Naturally Fractured Reservoir Models Using Static and Dynamic Data",	Garcia M., Gouth F., Gosselin O.	This paper presents an integrated approach that has been developed as a workflow for modelling naturally fractured reservoirs.
113618	2009	A Sensitivity Analysis for Effective Parameters on 2D Fracture-Network Permeability	A. Jafari, T. Babadagli.	This paper propose a new practical approach to estimate Fracture Network Permeability (FNP) using statistical and fractal characteristics of fracture networks.
131126	2010	"Effective Fracture Network Permeability: Comparative Study of Calculation Methods"	Cottereau N., Garcia M. Gosselin O. Vigier L.	First contribution to help clarify and quantify calculation methods, and approaches that are now available in commercial or in-house software tools for modelling equivalent flow properties of naturally fractured reservoir models.

SPE 426 (1963)

The Behavior of Naturally Fractured Reservoir

Authors: J. E. Warren, P. J. Root.

Contribution to the understanding of naturally fractured reservoirs:
An idealized model to study the characteristic behaviour of double porosity reservoir.

Objective of the paper:
To suggest a model, which will simulate the behavior of a formation with intermediate porosity.

Methodology used:
The method is based on the following assumptions:
The matrix material is homogeneous and isotropic, and contained within a systematic array of identical blocks
All of the secondary porosity is contained within an orthogonal system of continuous, uniform fractures which are oriented
Flow can occur between the primary and secondary porosities, but flow through the primary porosity cannot occur.

Conclusion reached:
Two parameters are sufficient to characterize the deviation of the behavior of a medium with double porosity from that of a homogenous, porous medium. One of the parameters ω, is a measure of the fluid capacitance of the secondary porosity and the other, λ is related to the scale of heterogeneity that is present in the system.

Comments:
This paper provides a basic for the study of naturally fractured reservoirs.

SPE 84078 (2003)

Practical Approach in Modeling Naturally Fractured Reservoir: A Field Case Study

Authors: Asnul B., Harun A., Maged H. A., Salem E., Hussein B., and Mohan K.,

Contribution to the understanding of naturally fractured reservoirs:
A practical approach in modeling of naturally fractured reservoirs, from geology to flow simulation.

Objective of the paper:
To develop a representative reservoir model to form the basis for reservoir management and long-term development planning.

Methodology used:
The approach used, was to generate alternate descriptions based on the stochastic techniques by integrating various data source from different disciplines
The hierarchical system was designed and implemented in designing the scenario for the multiple realizations in order to capture all possible uncertainties.
Matrix and Fracture properties are modelled separately and then integrated using newly developed techniques.
Streamline simulation technique was use for two purposes, namely ranking and upscaling
Flow simulation of single media model was use to simulate the naturally fractured reservoir

Conclusion reached:
Single media model is capable in simulating the naturally fractured reservoir.

Comments:
This paper provides a simplified approach in modelling naturally fractured reservoir.

SPE 101052 (2006)

History Matching for Determination of Fracture Permeability and Capillary Pressure

Authors: T. Gang and M. Kelkar

Contribution to the understanding of naturally fractured reservoirs:
This paper presents an integrated approach to history matching naturally fractured reservoirs by adjusting the fracture permeability of individual fractures and water/oil capillary pressure curves.

Objective of the paper:
To characterize fracture permeability and to estimate water/oil capillary pressure curves of naturally fractured reservoirs using production data.

Methodology used:
The adjoint method and an efficient direct solver were used to reduce CPU time for calculating the sensitivity-coefficient matrix.
A 2D synthetic case was used, with the fracture distribution from a Middle East reservoir, to validate the method.

Conclusion reached:
The water/oil capillary pressure can be estimated properly by use of the production data through the history-matching process.
The relation between the fracture permeability and grid permeability was assumed to be known—this may limit the application of this methodology.

Comments:
This is the first research work so far that has focused on estimating capillary pressure curves and fracture permeability by use of production data.

SPE 107525 (2007)

Fast and Efficient Modelling and Conditioning of Naturally Fractured Reservoir Models

Authors: M. Garcia, F. Gouth, and O. Gosselin,

Contribution to the understanding of naturally fractured reservoirs:
This paper presents an integrated approach that has been developed as a workflow for modelling naturally fractured reservoirs.

Objective of the paper:
To generate a reasonably complex models and methods in a consistent way with various fracturing and dynamic data in order to produce conditional model.

Methodology used:
Geostatistical modeling of fracture densities to honour well fracturing data and observed spatial trends.
Scale-dependent calculation of full permeability tensors, based on spatially periodic discrete fracture networks for horizontal within-layer permeabilities, and analytical solutions for vertical interlayer permeabilities.
Calibration of reservoir models using steady-state flow-based evaluation of equivalent well-test permeabilities.

Conclusion reached:
Modeling of naturally fractured reservoirs cannot be carried out without considering a multi-step approach.
Fracturing and explicative (geomechanical, seismic, structural or geological) information must be integrated to evaluate spatial and non-spatial model parameters on a directional fracture-set basis.

Comments:
The approach developed in this program is quite useful, since it enables you to build a realistic model that is not too simplistic and too complex.

SPE 113618 (2009)

A Sensitivity Analysis for Effective Parameters on 2D Fracture-Network Permeability

Authors: A. Jafari, T. Babadagli

Contribution to the understanding of naturally fractured reservoirs:
This paper propose a new practical approach to estimate Fracture Network Permeability (FNP) using statistical and fractal characteristics of fracture networks.

Objective of the paper:
To relate fracture-network characteristics to fracture network permeability for 2D random fracture networks quantitatively and to perform a sensitivity analysis using experimental-design technique to determine the fracture parameters that are most influential on the FNP.

Methodology used:
Different statistical and fractal characteristics of the networks were correlated to the measured FNPs using multivariable-regression analysis.
Twelve fractal (sandbox, box counting, and scanline fractal dimensions) and statistical (average length, density, orientation, and connectivity index) parameters were tested against the measured FNP for synthetically generated fracture networks for a wide range of fracture properties.

Conclusion reached:
The most influential fracture-network characteristics were indentified to be the box-counting fractal dimension of intersection points and fracture lines, and maximum touch with scanline in X- and Y-directions.
It was shown that among the four fracture parameters (length, density, orientation, and conductivity) and their combinations, the fracture density, length, and their combination have the most important impact on the FNP because they are the parameter that have a direct impact on obtaining a percolating network.
The conductivity of individual fractures starts becoming the dominating term over the network properties as the density and length values decrease, reaching a certain low range and the conductivity becomes high enough.

Comments:
The study in this paper was conducted in 2D fracture networks and may not be applicable to 3D fracture network.

SPE 131126 (2010)

Effective Fracture Network Permeability: Comparative Study of Calculation Methods

Authors: Cottereau N., Garcia M., Gosselin O., and Vigier L

Contribution to the understanding of naturally fractured reservoirs:
First contribution to help clarify and quantify calculation methods, and approaches that are now available in commercial or in-house software tools for modelling equivalent flow properties of naturally fractured reservoir models.

Objective of the paper:
To review and compare several equivalent permeability calculation methods.

Methodology used:
This work relies on benchmark case studies that involve three directional fracture sets with highly contrasting fracture conductivities from (10 to 1000mD).
Fracture lengths were taken to be greater than the gridblock sizes at which equivalent permeability tensors are to be assessed.

Conclusion reached:
Numerical methods offered by commercial products, based on 3D discrete fracture networks (DFN) to compute equivalent permeability tensors, are generally unable to manage full-field models, and that their simpler analytical methods are to be used with great caution

Comments:
This paper provides a basic for comparative benchmark case.

Appendix B: Sensitivity of Matrix Properties

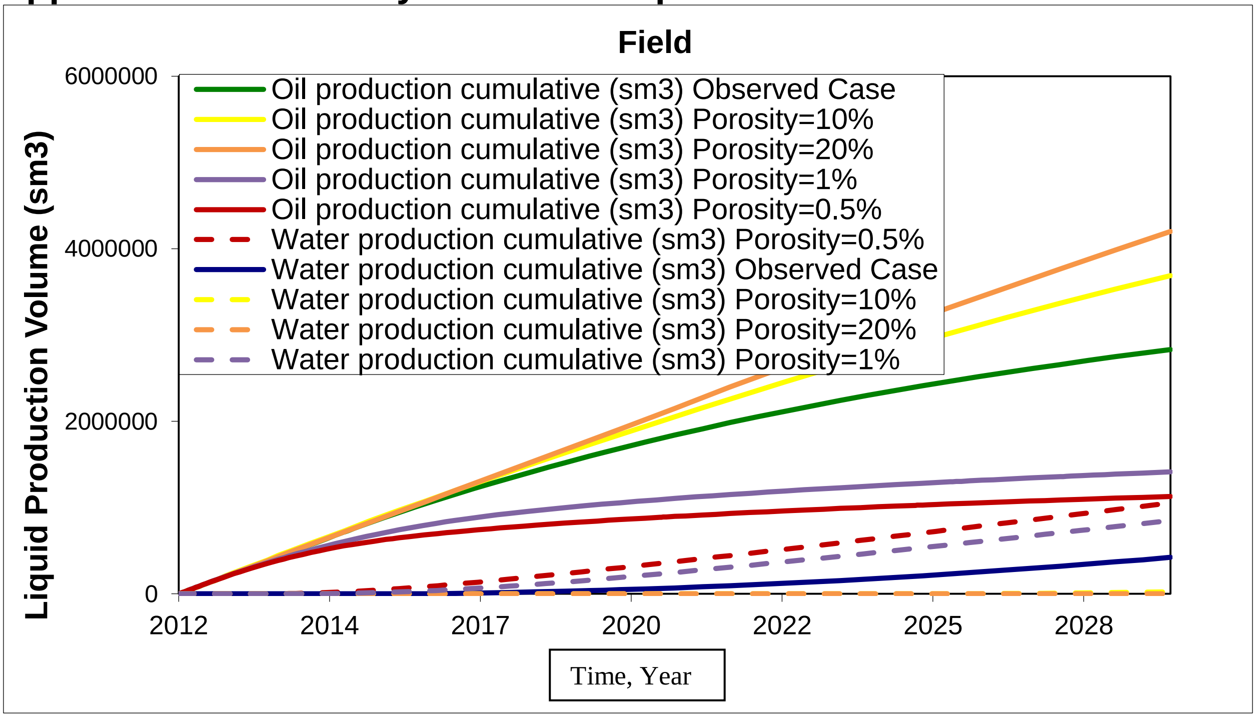

Figure B- 1: Cumulative oil and water production with different values of matrix porosity

Figure B-1, shows cumulative oil and water production with different matrix porosity ranging from 0.5% to 20%. From the figure, the matrix porosity has large impact on the field production.

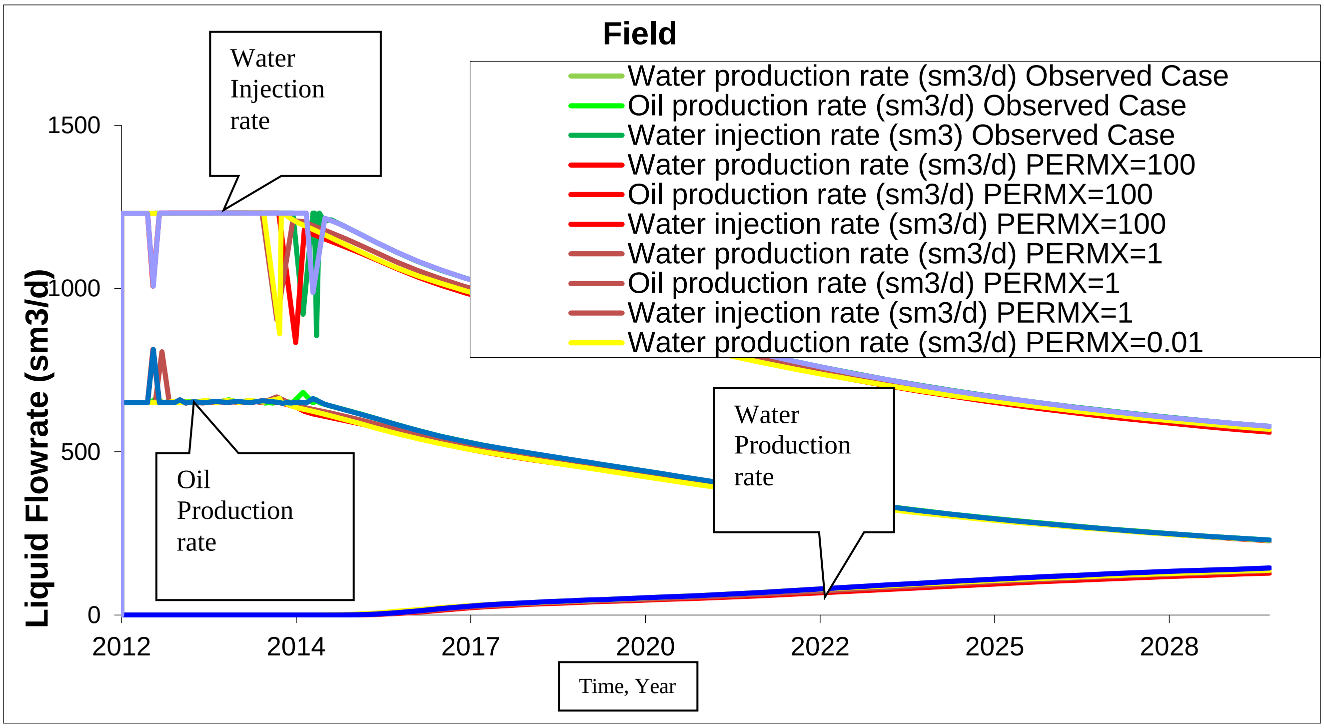

Figure B- 2: Cumulative oil and water production with different values of PERMX.

From figure 7, values of PERMX ranging from 0.01mD to 1000000mD has little or no effect on the field production.

Lastly, for different values of PERMY and PERMZ, ranging from 0.01 to 1000000mD, there was no change in the field production.

Appendix C: Experimental Design: Plot of Cumulative Oil Production

The figures below are plots of the 16 cumulative oil production used in the experimental design.

A3 High

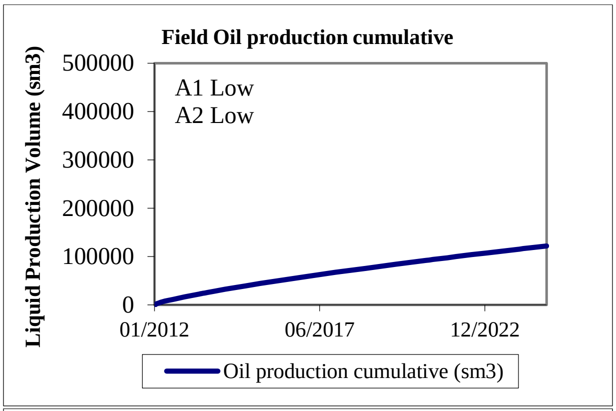

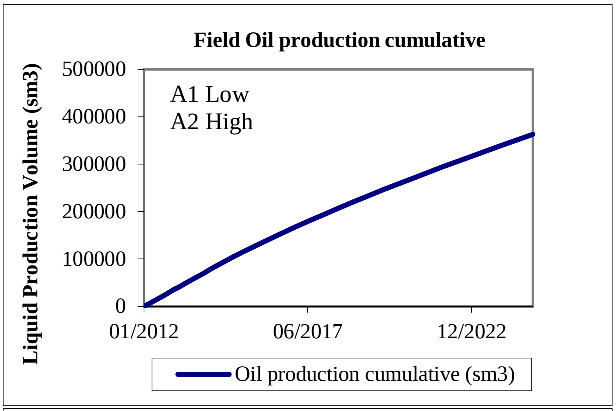

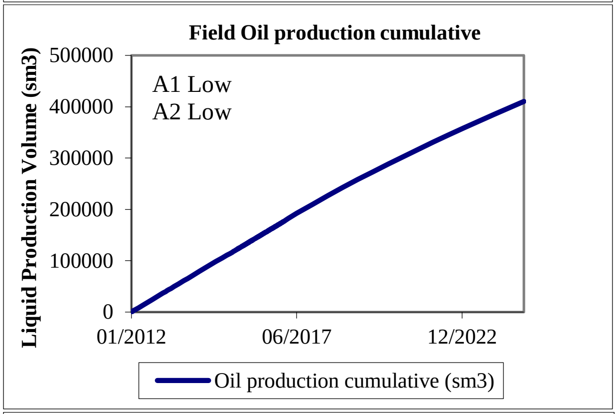

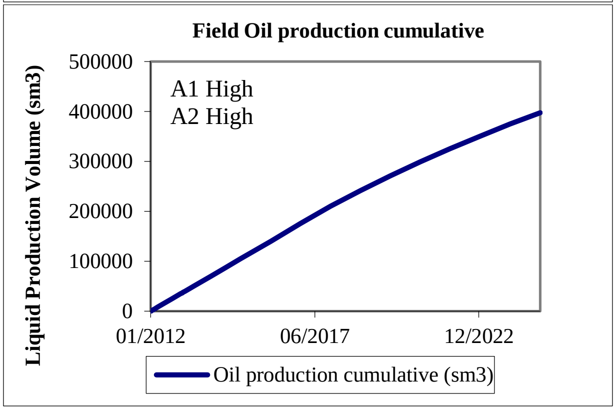

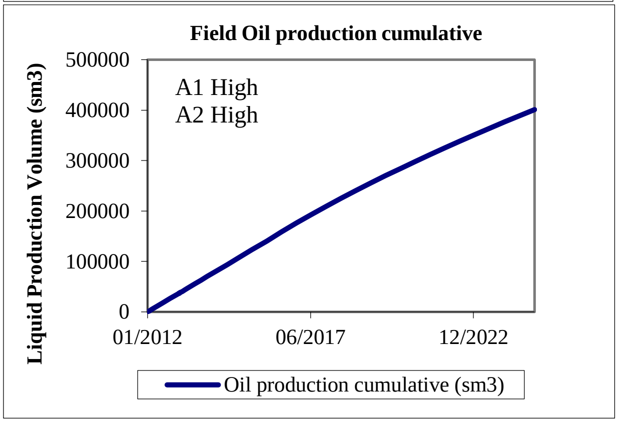

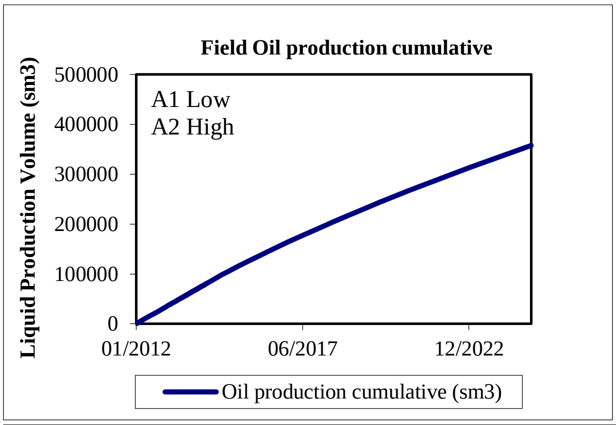

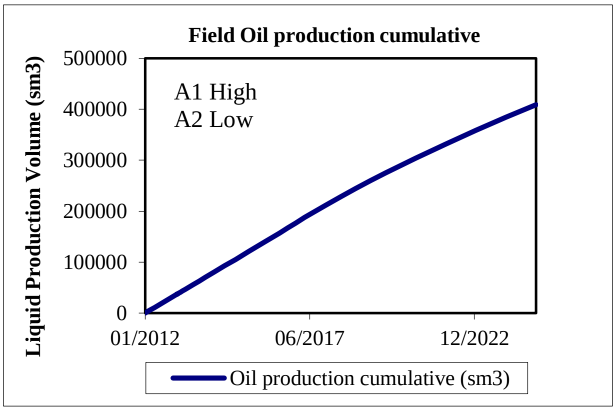

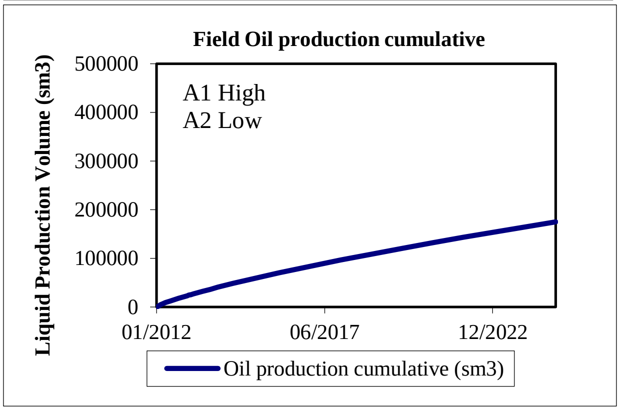

A3 Low

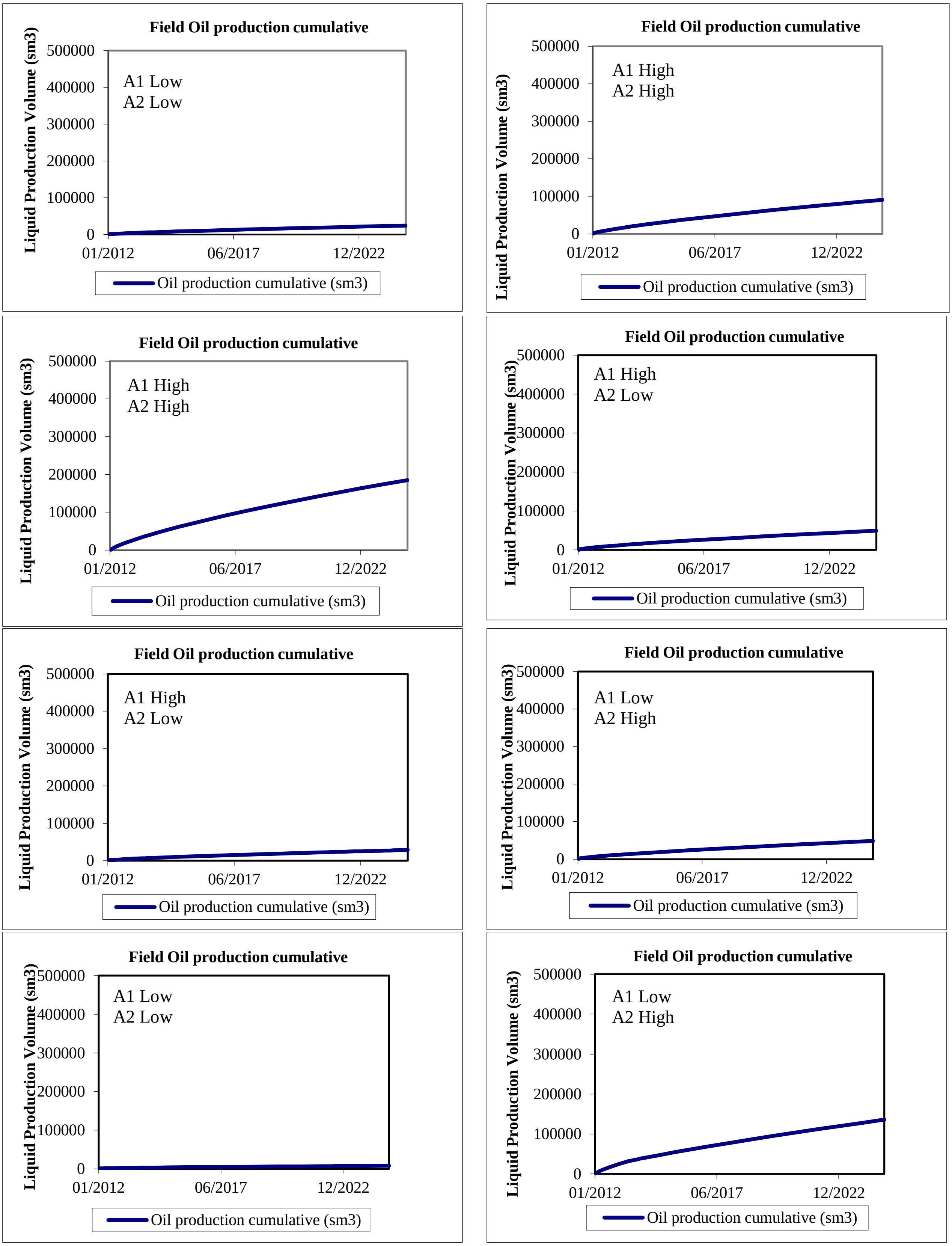
Field Oil production cumulative
Liquid Production Volume (sm3)
500000
400000
300000
200000
100000
0
01/2012
06/2017
12/2022
A1 Low
A2 Low
Oil production cumulative (sm3)
Field Oil production cumulative
A1 High
A2 High
Oil production cumulative (sm3)
Field Oil production cumulative
A1 High
A2 High
Oil production cumulative (sm3)
Field Oil production cumulative
A1 High
A2 Low
Oil production cumulative (sm3)
Field Oil production cumulative
A1 High
A2 Low
Oil production cumulative (sm3)
Field Oil production cumulative
A1 Low
A2 High
Oil production cumulative (sm3)
Field Oil production cumulative
A1 Low
A2 Low
Oil production cumulative (sm3)
Field Oil production cumulative
A1 Low
A2 High
Oil production cumulative (sm3)

Appendix D: Experimental Design: Plot of Cumulative Water Production

The figures below are plots of the 16 cumulative water production used in the experimental design.

A3 High

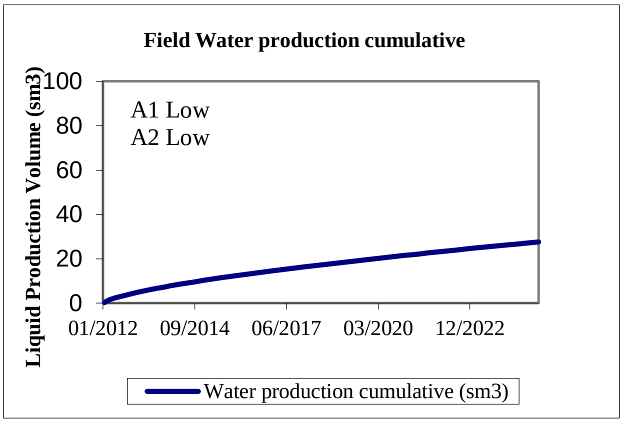

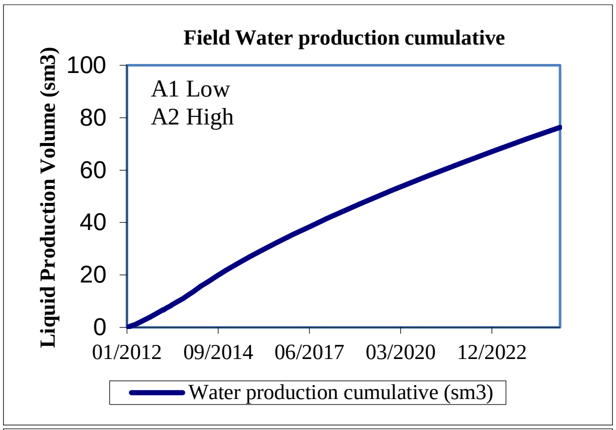

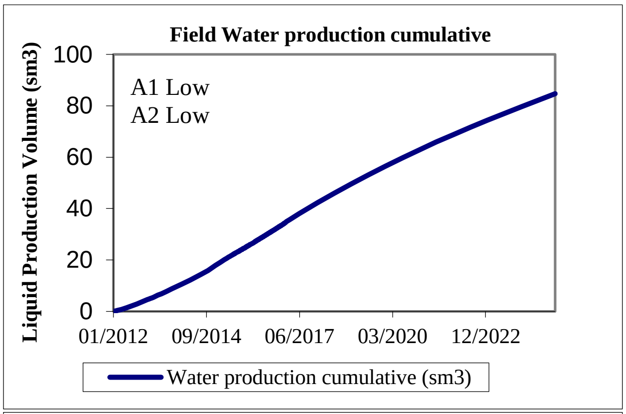

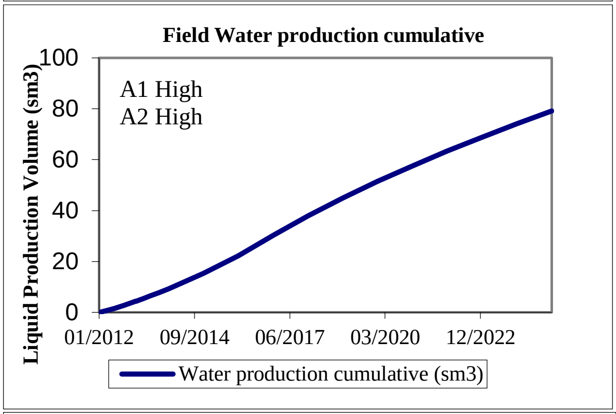

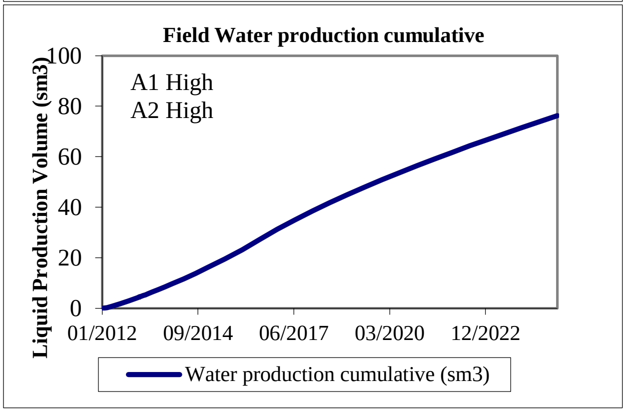

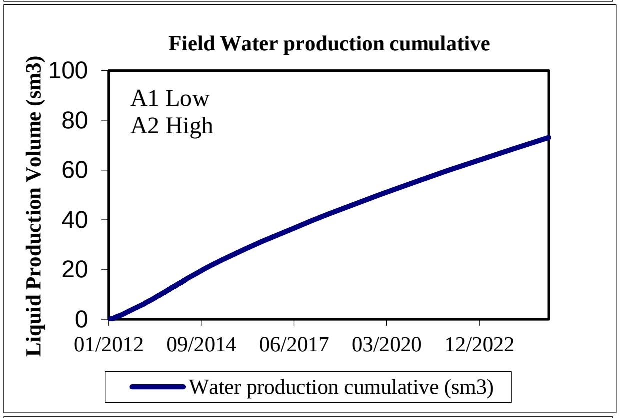

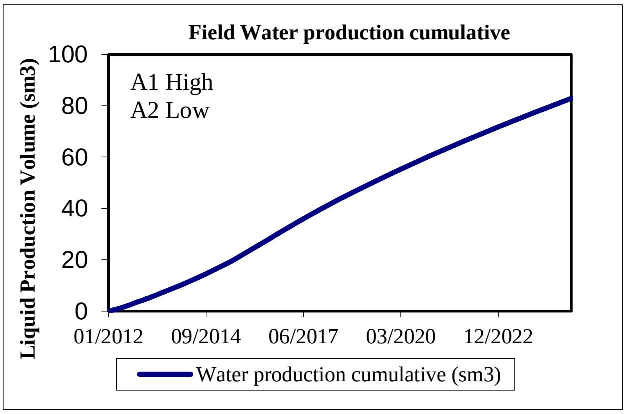

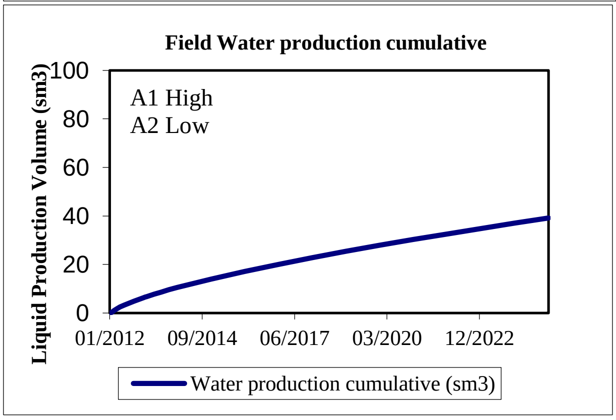

A3 Low

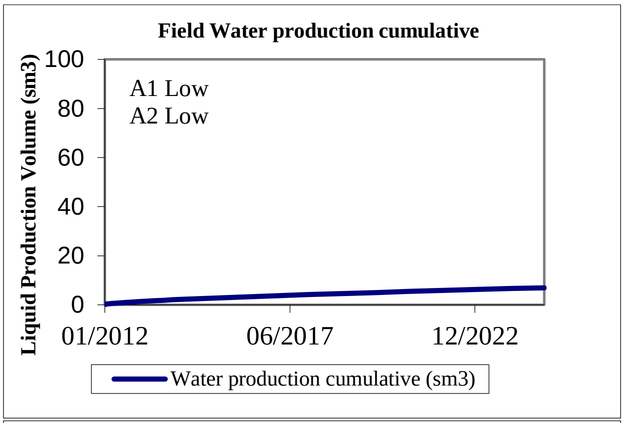
Field Water production cumulative
Liquid Production Volume (sm3)
100
80
60
40
20
0
01/2012
06/2017
12/2022
A1 Low
A2 Low
Water production cumulative (sm3)

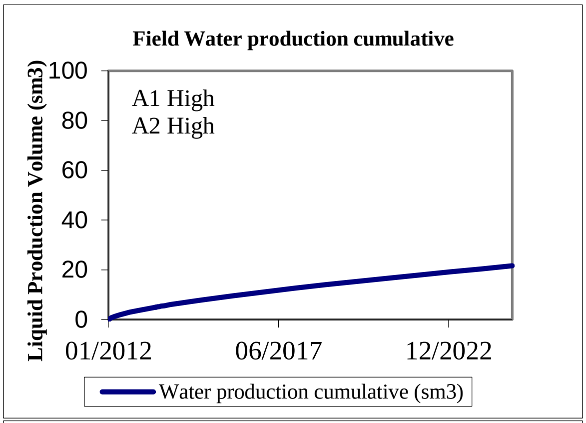
Field Water production cumulative
Liquid Production Volume (sm3)
100
80
60
40
20
0
01/2012
06/2017
12/2022
A1 High
A2 High
Water production cumulative (sm3)

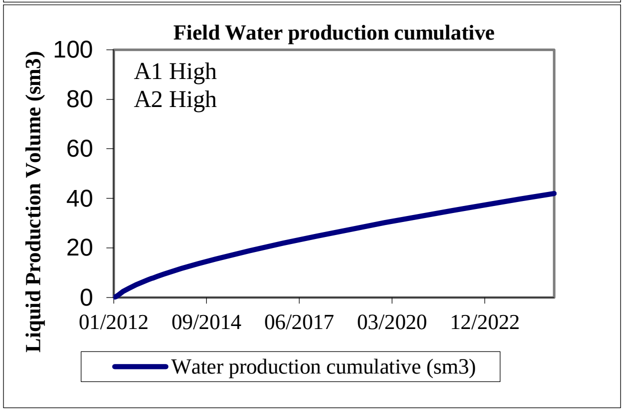
Field Water production cumulative
Liquid Production Volume (sm3)
100
80
60
40
20
0
01/2012
09/2014
06/2017
03/2020
12/2022
A1 High
A2 High
Water production cumulative (sm3)

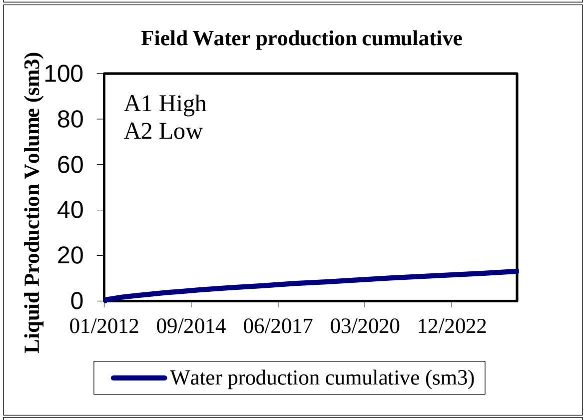
Field Water production cumulative
Liquid Production Volume (sm3)
100
80
60
40
20
0
01/2012
09/2014
06/2017
03/2020
12/2022
A1 High
A2 Low
Water production cumulative (sm3)

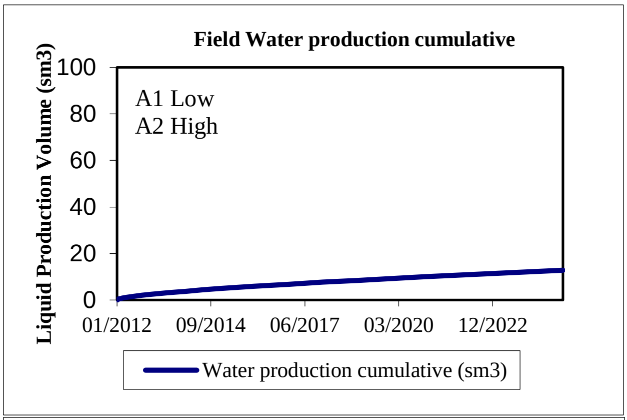
Field Water production cumulative
Liquid Production Volume (sm3)
100
80
60
40
20
0
01/2012
09/2014
06/2017
03/2020
12/2022
A1 Low
A2 High
Water production cumulative (sm3)

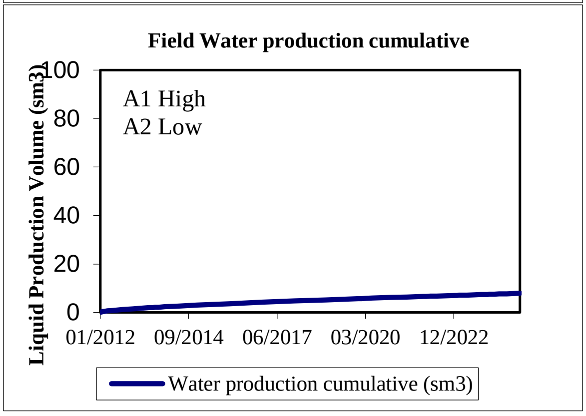
Field Water production cumulative
Liquid Production Volume (sm3)
100
80
60
40
20
0
01/2012
09/2014
06/2017
03/2020
12/2022
A1 High
A2 Low
Water production cumulative (sm3)

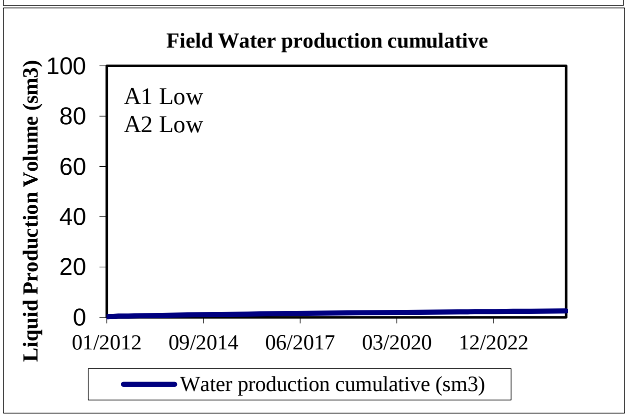
Field Water production cumulative
Liquid Production Volume (sm3)
100
80
60
40
20
0
01/2012
09/2014
06/2017
03/2020
12/2022
A1 Low
A2 Low
Water production cumulative (sm3)

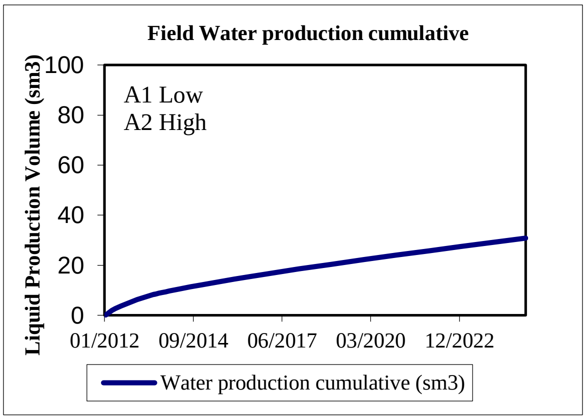
Field Water production cumulative
Liquid Production Volume (sm3)
100
80
60
40
20
0
01/2012
09/2014
06/2017
03/2020
12/2022
A1 Low
A2 High
Water production cumulative (sm3)

Appendix E: Experimental Design: Plot of Field Oil Production

The figures below are plots of the 16 field oil production used in the experimental design to obtain the length of plateau.

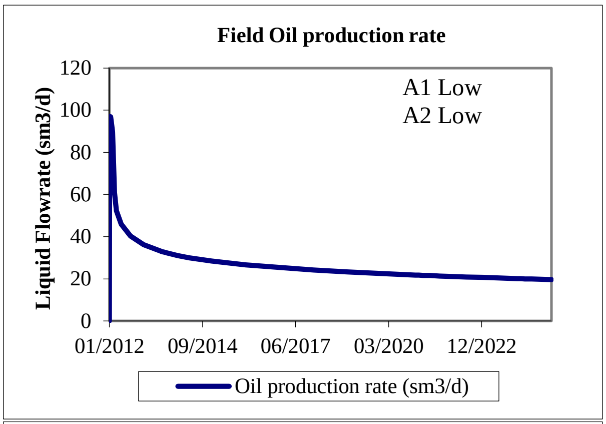

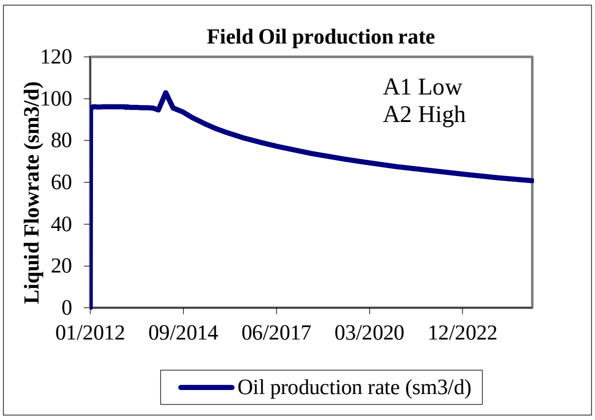

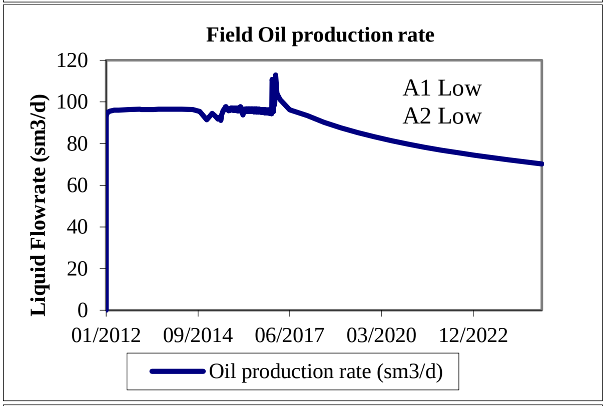

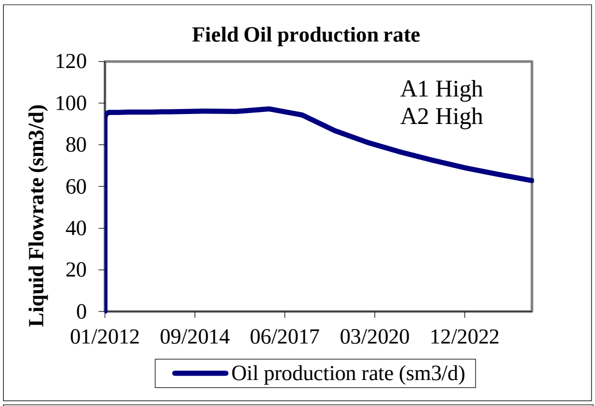

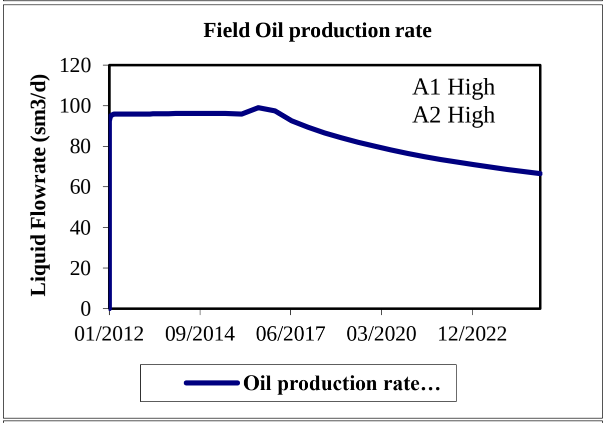

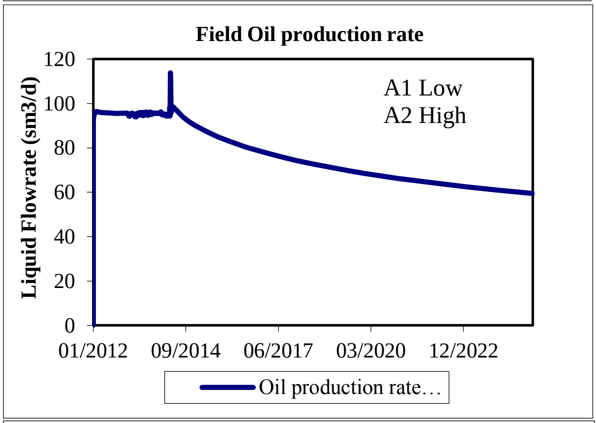

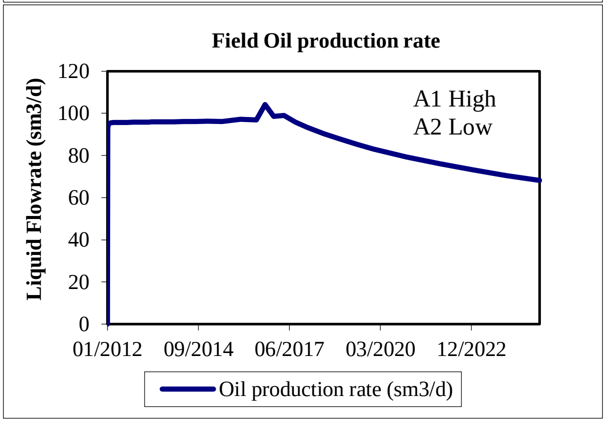

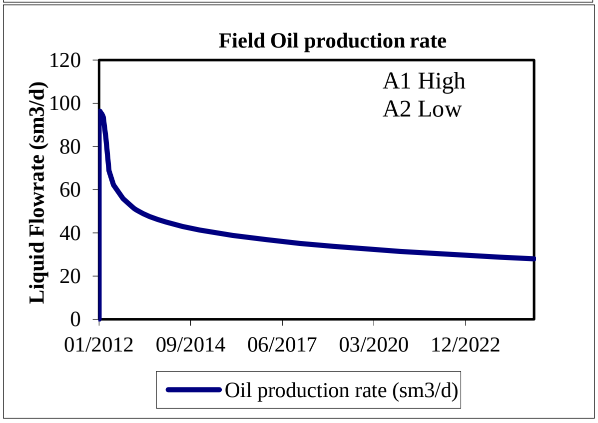

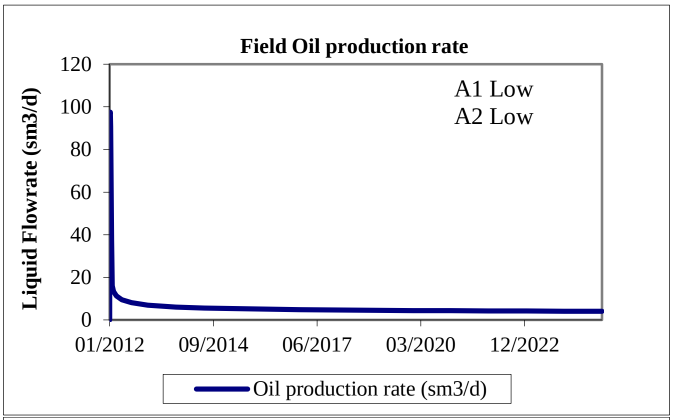
Field Oil production rate
Liquid Flowrate (sm3/d)
120
100
80
60
40
20
0
01/2012
09/2014
06/2017
03/2020
12/2022
A1 Low
A2 Low
Oil production rate (sm3/d)

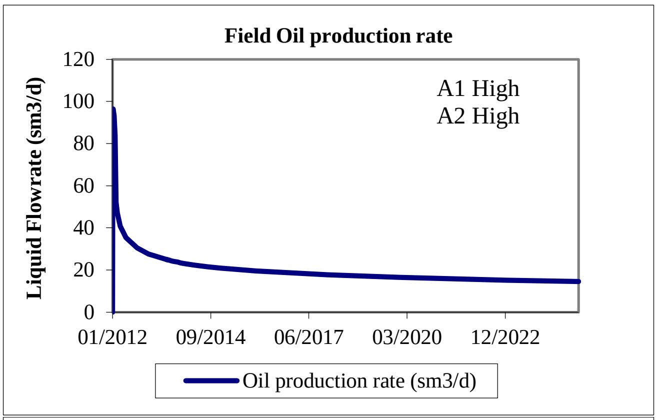
Field Oil production rate
Liquid Flowrate (sm3/d)
120
100
80
60
40
20
0
01/2012
09/2014
06/2017
03/2020
12/2022
A1 High
A2 High
Oil production rate (sm3/d)

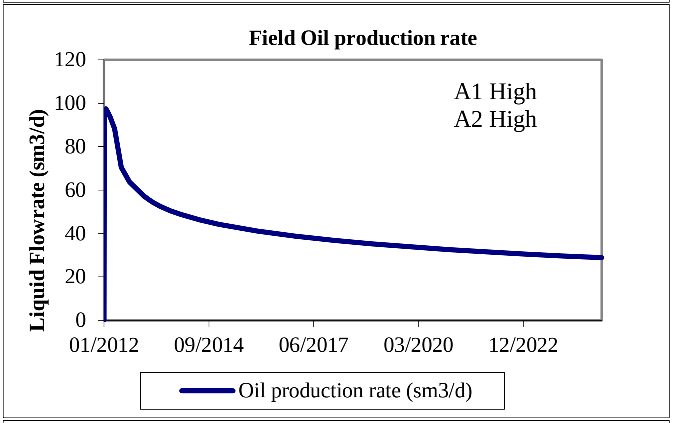
Field Oil production rate
Liquid Flowrate (sm3/d)
120
100
80
60
40
20
0
01/2012
09/2014
06/2017
03/2020
12/2022
A1 High
A2 High
Oil production rate (sm3/d)

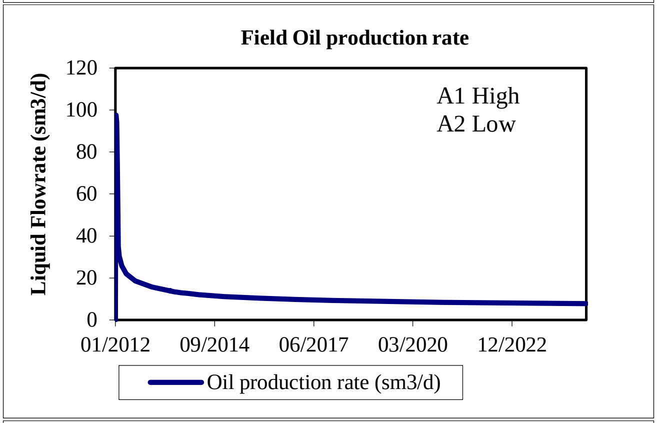
Field Oil production rate
Liquid Flowrate (sm3/d)
120
100
80
60
40
20
0
01/2012
09/2014
06/2017
03/2020
12/2022
A1 High
A2 Low
Oil production rate (sm3/d)

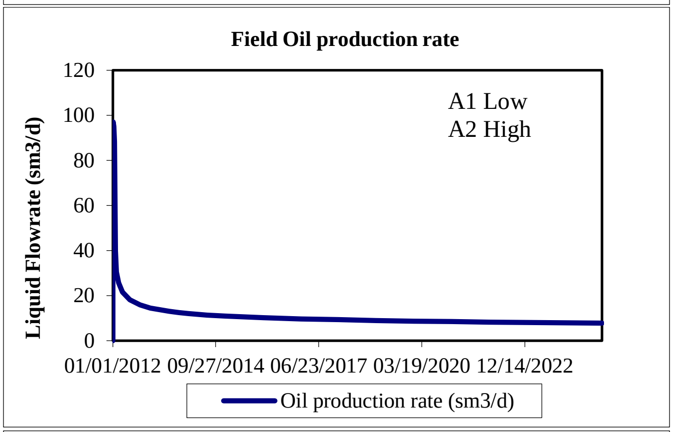
Field Oil production rate
Liquid Flowrate (sm3/d)
120
100
80
60
40
20
0
01/01/2012
09/27/2014
06/23/2017
03/19/2020
12/14/2022
A1 Low
A2 High
Oil production rate (sm3/d)

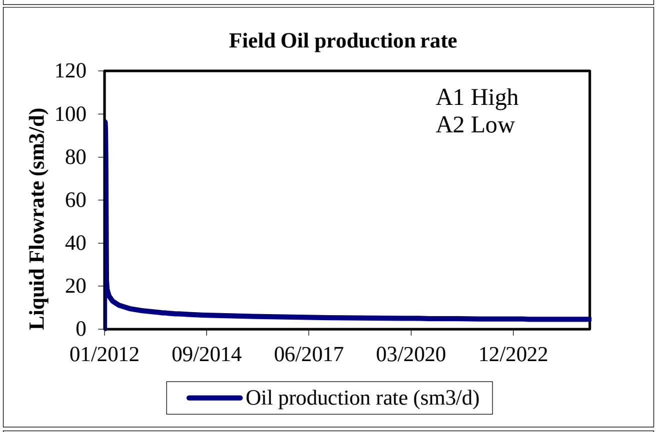
Field Oil production rate
Liquid Flowrate (sm3/d)
120
100
80
60
40
20
0
01/2012
09/2014
06/2017
03/2020
12/2022
A1 High
A2 Low
Oil production rate (sm3/d)

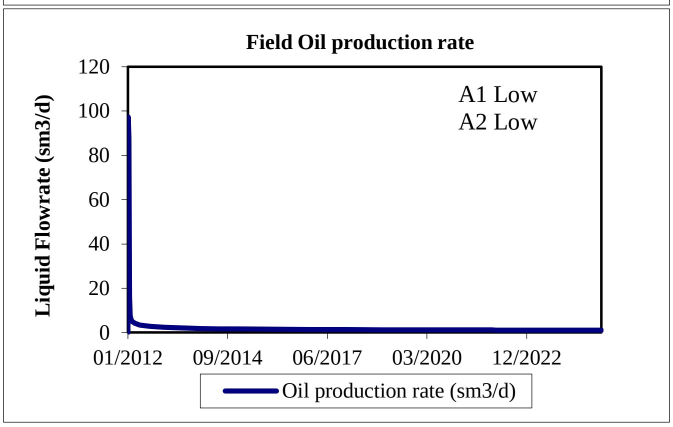
Field Oil production rate
Liquid Flowrate (sm3/d)
120
100
80
60
40
20
0
01/2012
09/2014
06/2017
03/2020
12/2022
A1 Low
A2 Low
Oil production rate (sm3/d)

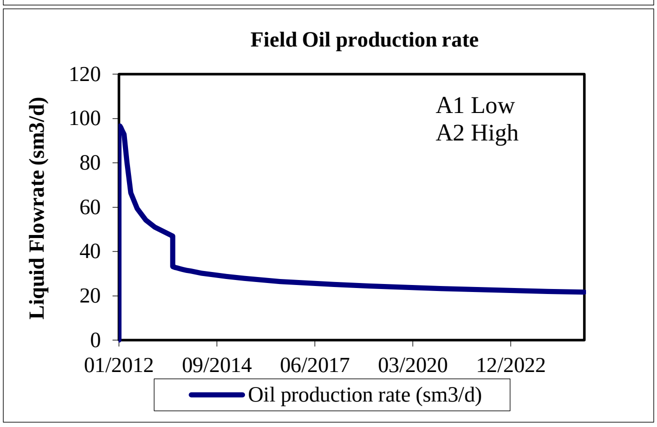
Field Oil production rate
Liquid Flowrate (sm3/d)
120
100
80
60
40
20
0
01/2012
09/2014
06/2017
03/2020
12/2022
A1 Low
A2 High
Oil production rate (sm3/d)